Original Article

MOLECULAR METABOLISM

Loss of FoxOs in muscle reveals sex-based differences in insulin sensitivity but mitigates diet-induced obesity

Christie M. Penniman [1,3], Pablo A. Suarez Beltran [1,3], Gourav Bhardwaj [1], Taylor L. Junck [1], Jayashree Jena [1], Kennedy Poro [1], Michael F. Hirshman [2], Laurie J. Goodyear [2], Brian T. O'Neill [1,*]

ABSTRACT

Objective: Gender influences obesity-related complications, including diabetes. Females are more protected from insulin resistance after diet-induced obesity, which may be related to fat accumulation and muscle insulin sensitivity. FoxOs regulate muscle atrophy and are targets of insulin action, but their role in muscle insulin sensitivity and mitochondrial metabolism is unknown.

Methods: We measured muscle insulin signaling, mitochondrial energetics, and metabolic responses to a high-fat diet (HFD) in male and female muscle-specific FoxO1/3/4 triple knock-out (TKO) mice.

Results: In male TKO muscle, insulin-stimulated AKT activation was decreased. AKT2 protein and mRNA levels were reduced and insulin receptor protein and IRS-2 mRNA decreased. These changes contributed to decreased insulin-stimulated glucose uptake in glycolytic muscle in males. In contrast, female TKOs maintain normal insulin-mediated AKT phosphorylation, normal AKT2 levels, and normal glucose uptake in glycolytic muscle. When challenged with a HFD, fat gain was attenuated in both male and female TKO mice, and associated with decreased glucose levels, improved glucose homeostasis, and reduced muscle triglyceride accumulation. Furthermore, female TKO mice showed increased energy expenditure, relative to controls, due to increased lean mass and maintenance of mitochondrial function in muscle.

Conclusions: FoxO deletion in muscle uncovers sexually dimorphic regulation of AKT2, which impairs insulin signaling in male mice, but not females. However, loss of FoxOs in muscle from both males and females also leads to muscle hypertrophy and increases in metabolic rate. These factors mitigate fat gain and attenuate metabolic abnormalities in response to a HFD.

Keywords FoxO; Gender differences; Sexual dimorphism; Insulin resistance; Muscle hypertrophy; High-fat diet; Glucose uptake; Diet-induced obesity

1. INTRODUCTION

Obesity-related insulin resistance affects both males and females, contributing to metabolic disease. Large epidemiologic studies show that diabetes and pre-diabetes are less prevalent in pre- and peri-menopausal females than males [1,2]. Although gender influences the prevalence and severity of metabolic diseases, males have historically been used in research to eliminate the confounding effects of gender. Male rodents fed a high-fat diet (HFD) develop insulin resistance in as few as three weeks, but females are more protected from metabolic disturbances caused by a HFD [3]. Given the increase in insulin resistance after menopause, researchers hypothesize that females are protected from metabolic syndrome due in part to estrogen [3]. Mounting evidence indicates that skeletal muscle insulin sensitivity and metabolism are increased in females compared to males, despite relative reductions in lean muscle mass and increased fat mass in females [4]. Indeed, more than 3,000 genes are differentially expressed in male and female skeletal muscle tissue, the primary site for insulin-stimulated glucose disposal [5].

Whole-body metabolism is impacted by many factors, including macronutrient intake, body composition, mitochondrial function, and basal and activity-induced energy expenditures. Body composition plays a critical role in basal metabolic rate and diet-induced obesity since metabolic improvements are seen in genetic models of muscle hypertrophy. Increasing muscle mass in both male and female mice by knockout of myostatin alleviates fat gain by increasing metabolic rate when normalized per animal [6]. Myostatin knockout ($Mstn^{-/-}$) also protected mice from fat gain and glucose intolerance caused by genetic forms of obesity, as demonstrated by crossing $Mstn^{-/-}$ mice with leptin deficient ob/ob or agouti (Ay/a) strains. Similarly, over-expression of a constitutively active AKT1 in muscle induced muscle hypertrophy and increased basal metabolic rate that protected mice

[1]Fraternal Order of Eagles Diabetes Research Center and Division of Endocrinology and Metabolism, Roy J. and Lucille A. Carver College of Medicine, University of Iowa, Iowa City, IA, 52242, USA [2]Section on Integrative Physiology and Metabolism, Joslin Diabetes Center, Harvard Medical School, Boston, MA 02215, USA

[3] Christie M. Penniman and Pablo A. Suarez Beltran contributed equally to this work.

*Corresponding author. University of Iowa, 169 Newton Road, 3314 PBDB, Iowa City, IA, 52242, USA. E-mail: Brian-Oneill@uiowa.edu (B.T. O'Neill).

Received September 6, 2019 • Accepted October 1, 2019 • Available online 10 October 2019

https://doi.org/10.1016/j.molmet.2019.10.001

from diet-induced obesity and insulin resistance [7]. Downstream of AKT, inhibition of FoxO proteins controls muscle size by limiting protein degradation, but whether a common intramyocellular mechanism involving FoxOs accounts for the coordination of growth and basal metabolic rate is not known.

FoxOs are ubiquitously expressed transcription factors that control cellular differentiation, muscle growth, metabolism, and tumor suppression pathways [8]. FoxOs are known to mediate muscle atrophy by regulating expression of protein degradation genes, including Atrogin1, MuRF-1, and autophagy genes [9–11]. FoxOs are directly inhibited by the actions of insulin and IGF-1, and we have previously shown that they mediate muscle atrophy due to deletion of insulin receptors and IGF-1 receptors [12,13]. Insulin acts through its tyrosine kinase receptor to mediate metabolic changes and cellular growth. The insulin receptor (IR) and the closely related IGF-1 receptor (IGF1R) have overlapping roles in mediating muscle growth, and glucose homeostasis [12,14]. Both IR and IGF1R activate the PI3-kinase/AKT, and MAPK/ERK pathways to influence cellular function. In the fed state, insulin increases glucose uptake in muscle by activation of AKT, leading to Glut4 glucose transporter translocation to the plasma membrane, and insulin inhibits protein degradation by AKT-mediated FoxO suppression [13]. In states of insulin resistance, insulin-mediated AKT activation is reduced in skeletal muscle, and glucose uptake is impaired. A recent study showed that FoxO inactivation in muscle decreased glucose uptake [15]. However, the role of FoxOs in muscle glucose metabolism or regulation of obesity-induced insulin resistance has not been fully explored.

Muscle mitochondrial dysfunction is associated with obesity and insulin resistance in peripheral tissues and may contribute to type 2 diabetes [16]. Previous studies have reported that diet-induced obesity can cause structural anomalies in both the subsarcolemmal and intramyofibrillar mitochondria in mouse muscle [17]. Humans and mice fed a HFD show similar transcriptional responses in muscle with decreases in mitochondrial biogenesis (PGC-1α) and oxidative phosphorylation transcripts [18,19]. However, the role of diet-induced obesity in muscle mitochondrial dysfunction remains controversial. Indeed, other investigators have discerned no differences in muscle oxidative capacity with diet-induced or genetic obesity, but indicated that lack of insulin signaling—as occurs in patients with insulin-deficient diabetes—is associated with mitochondrial dysfunction [20]. Furthermore, the role of FoxO in muscle mitochondrial adaptations to diet-induced obesity is unknown.

We explored the role of FoxOs in muscle insulin sensitivity and glucose metabolism in male and female mice on normal chow (NC) and when exposed to a HFD. In both male and female mice, we found that muscle-specific FoxO 1/3/4 triple knockout (TKO) led to increased muscle size, without differences in whole-body glucose metabolism on NC. However, male TKO mice did show muscle insulin resistance, manifested by decreased AKT phosphorylation and decreased insulin-stimulated glucose uptake in glycolytic EDL muscle. These changes in insulin action were associated with decreased mRNA and protein expression of AKT2 in muscle from male TKO mice, but not from female mice. Both male and female TKO mice gained less fat mass and showed improved glucose levels and glucose homeostasis on a HFD, effects that were independent of muscle insulin sensitivity. In females, this was due to increased energy expenditure in TKO mice, which was proportional to the increase in lean muscle mass and led to reduced intramyocellular triglyceride accumulation. Thus, deletion of FoxOs in skeletal muscle reveals sex-based differences in AKT2 expression that are associated with impaired insulin action in muscle from male, but not female, mice. Nonetheless, loss of FoxOs induces muscle hypertrophy in both males and females, leading to increased energy expenditure which mitigates fat gain and metabolic complications of a HFD.

2. MATERIALS AND METHODS

2.1. Animal care and use

Animal studies were performed according to protocols approved by the Institutional Animal Care and Use Committee (IACUC) at the University of Iowa and Joslin Diabetes Center. Both male and female mice were used for all studies, unless otherwise stated. FoxO-TKO mice (muscle-specific deletion of FoxO1, FoxO3, and FoxO4) were generated using ACTA1-Cre (Jackson Laboratory, stock number 006149). FoxO1/3/4 triple floxed mice were provided by Dr. C. Ronald Kahn, as previously described [12]. Littermate controls were used for all experiments as the mice are on a mixed background containing C57Blk6, C57Blk6J, and 129 strains. Unless otherwise specified, all animals were allowed *ad libitum* access to food and water and were sacrificed at 09:00.

2.2. Insulin signaling

Mice were fasted for 16 h in order to drive glucose levels as low as possible to accurately measure insulin signaling. They were then anesthetized with a 120–300 mg/kg IP injection of Avertin and were injected with 5U of insulin via the vena cava. After 3 min, the mice were sacrificed, and their tissues were collected; all tissues were simultaneously frozen 10 min after injection.

2.3. HFD study

At 8–10 weeks of age, FoxO-TKO mice and their littermate controls were either maintained on NC (NIH-31 irradiated modified mouse/rat diet 7913) or a HFD (Open source Diet, D12492; Research Diets) containing 60% calories from fat for 18 weeks. The NC diet had an energy density of 3.1 kcal/g while the HFD had an energy density of 5.21 kcal/g. Bodyweight and body composition were measured by nuclear magnetic resonance (NMR) using an LF-50 NMR with help from the University of Iowa Metabolic Core. Glucose tolerance tests (GTT) were performed at 7 and 15 weeks, and insulin tolerance tests (ITT) were performed at 8 and 16 weeks. During the 14th week, the mice were singly housed in metabolic cages for indirect calorimetry and behavioral studies.

2.4. Glucose tolerance test (GTT) and insulin tolerance test (ITT)

For GTTs, mice were fasted overnight for 16 h. Baseline whole blood glucose levels were measured, and blood samples were collected for serum extraction. Each mouse was given an IP injection of 2 mg dextrose/g body weight. Whole blood glucose levels were measured using a glucose meter at 15, 30, 60, and 120 min post-injection. For ITTs, mice were fasted for 2 h. Baseline glucose levels were measured before IP injection with 1mU/g body weight of regular human insulin (Novolin brand). Whole blood glucose levels were measured at 15, 30, 60, 90, and 120 min post-injection.

2.5. Ex vivo muscle glucose uptake

Glucose uptake was measured in the EDL and soleus muscles, as previously described [14,21]. Briefly, mice were fasted starting at 22:00 and muscle harvested the next day between 10:00 and 13:00. Isolated EDL and soleus muscles were incubated with resting tension in Krebs Ringer Buffer (KRB) containing (in mM) 117 NaCl, 4.7 KCl, 2.5 $CaCl_2$, 1.2 KH_2PO_4, 1.2 $MgSO_4$, and 24.6 $NaHCO_3$ at pH 7.5. Muscles were pre-incubated in KRB with 2 mM pyruvate, 7 mM mannitol, with or without 5 mU/ml of insulin for 30 min. Muscles were transferred to transport KRB for 10 min that contained 1 mM 2-deoxyglucose and

7 mM mannitol with 1.5 μCi/mL [^{3}H] 2-deoxyglucose (Perkin Elmer NET549250UC) and 0.3 μCi/mL [^{14}C] mannitol (Perkin Elmer NEC852050UC) with or without 5 mU/ml of insulin. Muscles were snap-frozen in liquid nitrogen after 10 min, weighed, then digested in 250 μl of 1 M NaOH for 20 min at 50 °C. Tubes were cooled and neutralized with 250 μl of 1 M HCL. Radioactivity in aliquots of the digested muscle was determined by liquid scintillation counting for dual [^{3}H] and [^{14}C] labels, and the accumulation of [^{3}H]-2-deoxyglucose was calculated after correcting for extracellular space with [^{14}C]-mannitol and normalizing to muscle weight.

2.6. Indirect calorimetry in metabolic cages

Mice were individually housed in Promethion metabolic cages (Sable Systems) for 6 days with their respective feeds. During the first 30 h of acclimation, data were recorded, but excluded from the analysis. Over the next 48 h, the mice were *ad libitum* fed over 12-hour dark and light cycles, followed by a 24 h fast, then a 24-hour re-feed period. Metabolic cage experiments were done in conjunction with the University of Iowa Metabolic phenotyping core.

2.7. Triglyceride measurements

Triglycerides were measured in serum samples using the Sigma Serum Triglyceride Determination Kit (Catalog Number TR0100), according to the manufacturer's protocol. For tissue triglyceride levels, liver or quadriceps tissues were homogenized in a 2:1 chloroform: methanol mixture at a ratio of 1:19 tissue weight to volume. Saline was added to homogenate in a 1:5 ratio to perform a Folch extraction. A 20 ul organic layer sample was evaporated under nitrogen and triglyceride concentrations were measured using Sigma triglyceride kit using an appropriate standard for quantification.

2.8. Insulin concentrations

Insulin concentrations from serum samples were measured using the Crystal Chem Ultra-Sensitive Mouse Insulin ELISA Kit (Catalog # 90080), according to the manufacturer's protocol.

2.9. Mitochondrial isolation

Muscle mitochondria were isolated by differential centrifugation from mixed quadriceps/gastrocnemius muscle, as previously described [22].

2.10. Mitochondrial function assays

Mitochondrial function and ATP production were measured in permeabilized soleus fibers or isolated muscle mitochondria using an Oroboros Oxygraph similar to previous methods [23]. Briefly, the soleus muscles were dissected and immediately placed into ice-cold Buffer X containing 7.23 mM K_2EGTA, 2.77 mM CaK_2EGTA, 20 mM Imidazole, 0.5 mM DTT, 20 mM Taurine, 5.7 mM ATP, 14.3 mM creatine monophosphate, 6.56 mM $MgCl_2$—$6H_2O$, 50 mM MES [2-(N-morpholino) ethanesulfonic acid], with a pH of 7.1. The fibers were manually dissociated and separated into three bundles using blunted needles under a dissecting microscope, then permeabilized in Buffer X containing 50 μg/ml saponin for 40 min on ice. Fiber bundles were placed in Buffer Z containing 105 mM K-MES, 30 mM KCl, 10 mM KH_2PO_4, 5 mM $MgCl_2$—$6H_2O$, 2.5 mg/ml BSA, 1 mM EGTA, 20 μM Blebbistatin, 20 mM Creatine monohydrate, pH 7.4 on ice until use. For respiration measurements, fibers (~2 mg) were placed in 2.5 mL of Buffer Z at 30 °C and respiration was determined using an Oroboros oxygraph with the following substrates (and concentrations): Malate — 2 mM, Pyruvate (where specified) — 5 mM, Palmitoyl-carnitine (where specified) — 60 μM, Glutamate (where specified) — 5 mM, ADP (State 3 when added) — 1 mM, Succinate — 5 mM, Rotenone — 10 μM, Oligomycin — 10 μg/mL, FCCP — 10 μM. ATP production was measured in Buffer Z, containing 0.5 mg/ml BSA instead of 2.5 mg/ml. To monitor ATP production, ATP was converted to NADPH by addition of 4 mM glucose, 200 μM NADP+ (Sigma N0505), 50 μM P^1,P^5-Di (adenosine-5′) pentaphosphate pentasodium salt (Sigma D4022), and 10 μL/mL of a Hexokinase/Glucose-6-Phosphate Dehydrogenase mixture (Sigma 10127825001) to Buffer Z and monitored in a Horiba fluorometer Ex/Em (345 nm/460 nm). Respiration of isolated mitochondria was performed using 75 μg/mL of mitochondrial protein in a "Respiration Buffer" containing 120 mM KCl, 5 mM KH_2PO_4, 2 mM $MgCl_2$, 1 mM EGTA, 3 mM HEPES, 0.3% BSA fatty acid-free, pH 7.2, as described previously [24].

2.11. H_2O_2 assays

H_2O_2 was measured in isolated mitochondria, as previously described [24]. Briefly, H_2O_2 production was measured in 100 μg/mL of mitochondrial protein in respiration buffer containing (in mM) 120 KCl, 5 KH_2PO_4, 2 $MgCl_2$, 1 EGTA, 3 HEPES [pH 7.2] with 0.3% fatty acid—free BSA, 20 μM Ampliflu Red (Sigma 90101) and 5unit/ml Horseradish peroxidase. H_2O_2 reacts with HRP and Ampliflu Red to produce a fluorescent product Resorufin. To clamp the ADP concentration at low physiologic levels, 5 mM 2-deoxyglucose and 5 unit/ml Hexokinase were added to the buffer, which constantly utilizes ATP and regenerates ADP, as previously described [24]. This was monitored in a microplate fluorometric reader at 37 °C with Ex/Em (530 nm/590 nm) over 20 min.

2.12. Citrate synthase and β-hydroxyacyl-CoA-dehydrogenase (HADH) assays

Quadricep tissue was homogenized in buffer containing 250 mM sucrose, 20 mM Tris, 40 mM KCl, and 2 mM EGTA at a pH of 7.4 to measure citrate synthase and HADH activity, as previously described [25,26]. Briefly, citrate synthase was measured using 5 μg of homogenate protein in a final solution of 200 μl containing 200 mM Tris with a pH of 8.0, 0.2% vol/vol Triton X-100, 100 μM of 5,5′-Dithiobis (2-nitrobenzoic acid) (DTNB), 10 mM Acetyl-CoA, and 0.5 mM oxaloacetic acid which started the reaction. The reaction was monitored for an increase in absorbance at 412 nm for 3 min [25]. The HADH activity was measured using 10 μg of the sample in a final solution of 200 μl at a 7.4 pH, containing 20 mmol/L Tris, 1 mmol/L EGTA, 1 mmol/L KCN, 0.15 mmol/L NADH and 0.05 mmol/L Acetoacetyl-CoA which started the reaction. The reaction was monitored at 340 nm for 4 min with a spectrophotometer.

2.13. Histology

Dissected tissues were stored in 10% formalin until processing. The tissues were embedded in paraffin, sectioned, and stained with hematoxylin and eosin (H&E), then photographed using a light microscope at the University of Iowa Central Microscopy Research Facility.

2.14. Quantitative RT-PCR

Total mRNA was isolated from liver or muscle using Trizol (Thermo Fisher) and adipose tissues using Qiazol (Qiagen) according to the manufacturer's protocol. mRNA was converted to cDNA (Applied Biosystems # 4368814). Quantitative RT-PCR was performed on the liver and adipose tissue samples using the Bimake 2x SYBR Green qPCR Master Mix (catalog #B21203), with primers for target genes listed in Supplemental Table 1. TBP, GAPDH, and Rpl39 mRNA levels were measured in each group and analyzed to determine the gene which best represented the total mRNA level. TBP was used for normalization unless otherwise specified.

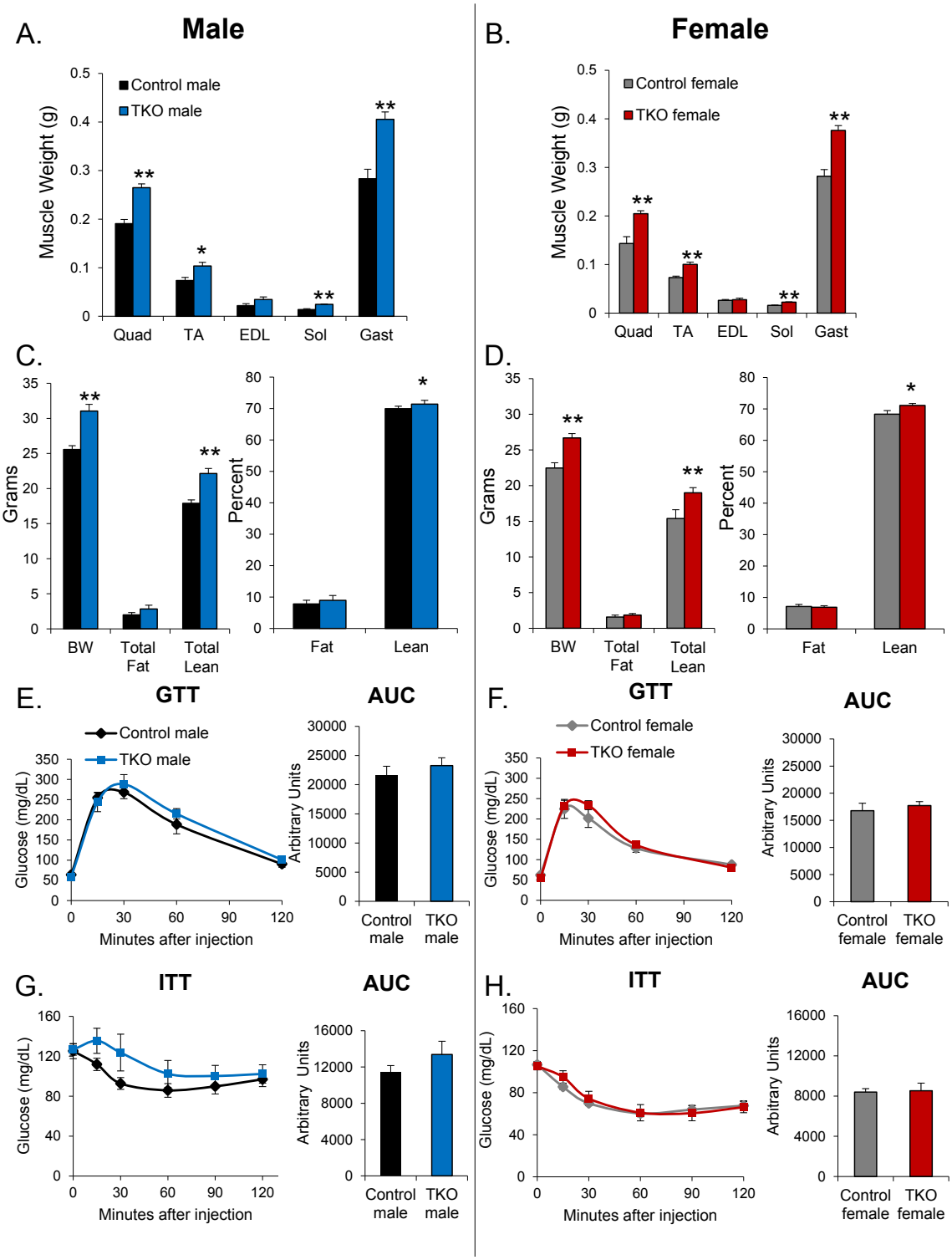

Figure 1: Muscle-specific FoxO deletion increases muscle mass equally in male and female mice and maintains glucose and insulin tolerance. Mice were studied between 16 and 22 weeks of age. The absolute weight of dissected muscles from both hindlimbs of male (A) and female (B) FoxO-TKO and littermate control mice (n = 5 per group in males and 10 per group in females). Body composition of male (C) and female (D) mice showing body weight (BW), total fat and lean mass, and % fat and % lean mass (n = 11–14 per group in both sexes). Glucose excursions and area under the curve (AUC) of glucose tolerance tests (GTT) in male (E) and female (F) mice (n = 11–14 per group in both sexes). Glucose excursions and AUC of insulin tolerance test (ITT) in male (G) and female (H) mice (n = 11–14 per group in both sexes). *-$p<0.05$, **-$p<0.01$ t-test. (Quad – median belly of the rectus femoris from quadriceps, TA – tibialis anterior, EDL – extensor digitorum longus, Sol - soleus, and Gast – gastrocnemius).

2.15. Western analysis

The muscle was homogenized in RIPA buffer (Millipore) with protease and phosphate A and B inhibitors (Bimake). Lysates were subjected to SDS-PAGE and blotted using the antibodies listed in Supplemental Table 2.

2.16. Statistics

All data are presented as means ± SEMs. Two-tailed t-tests were performed for all two-group comparisons. Two-way ANOVA with Tukey's test for multiple comparisons was performed using GraphPad Prism software for four or more groups to determine significance, with $p < 0.05$ being significant. If the Tukey's test for multiple comparisons did not reach $p < 0.05$, then ANOVA main effects were presented with a line over all data to indicate that individual groups were not statistically different from each other.

3. RESULTS

3.1. Muscle-specific FoxO deletion increases muscle mass equally in male and female mice and maintains glucose and insulin tolerance

To determine whether muscle-specific FoxO deletion impacted sex-based differences in body composition and insulin action, we measured morphologic and metabolic parameters in FoxO-TKO male and female mice along with littermate controls. First, we confirmed that FoxO1, FoxO3, and FoxO4 expression was decreased in muscle from FoxO-TKO males and females relative to controls (Supp Figs. S1A–S1B). TKO mice showed the same degree of increased muscle mass in both males and females (Figure 1A–B). Interestingly, mixed-fiber muscle groups of Quad, TA, and Gastroc showed a consistent 35–45% increase in absolute muscle size in TKO, compared to littermate controls, in both males and females. However, the EDL muscle showed relatively little change in mass, while the soleus muscles were markedly enlarged in TKO by 42–78%, relative to controls. Body composition by NMR showed a significant difference in total body weight which was accounted for by increased lean mass in both male and female mice (Figure 1C–D). Other dissected tissue weights were not changed in TKO mice relative to controls, although female TKOs did show a mild, but significant, increase in liver weight (Supp Figs. S1C–S1D).

To examine the differences in glucose homeostasis in male and female mice, we performed GTTs and ITTs. We observed no differences in glucose levels or area under the curve (AUC) during the GTT between TKO mice and littermate controls (Figure 1E–F). In agreement with previous observations [3], fasted glucose levels and glycemic excursions were lower in females compared to males, regardless of genotype. While insulin tolerance tended to be impaired in male TKO mice relative to controls, this difference was not significant (Figure 1G). Glucose excursions and AUC during ITT were unchanged in female TKOs compared to controls (Figure 1H). These data demonstrate that, while deletion of FoxOs in muscle led to increased muscle mass in both males and females, it did not alter whole-body glucose or insulin tolerance.

3.2. FoxO deletion reveals sex-based differences in muscle insulin signaling and AKT2 expression

We investigated insulin action in muscle from both male and female mice in control and TKO groups. To test insulin signaling, we determined phosphorylation of insulin signaling targets in TA muscle from fasted mice treated with high dose (5U) insulin or saline via vena cava injection. Phosphorylation of the insulin receptor and IGF-1 receptor (IR/IGF1R) was decreased in the TA from insulin-treated male TKO mice, compared to controls (Figure 2A). However, when normalized to total IR, the p-IR/IGF1R per total IR ratio was increased in male TKO mice (Figure 2B). This increased ratio was due to a decrease in total IR expression in TA from male TKOs (Supp. Figs. S2A–S2B). Downstream phosphorylation of AKT was impaired in male TKO mice by nearly 50% (Figure 2C), despite a trend toward decreased total AKT levels in male TKO (Supp. Figs. S2A–S2B). By contrast, female mice showed robust increases in p-IR/IGF1R and p-AKT after insulin stimulation, with no differences between insulin-stimulated muscle from TKO females compared to control females (Figure 2D–F). The preserved insulin signaling occurred despite mild decreases in IR expression in TA muscle from female TKOs, relative to female controls (Supp. Figs. S2C–S2D).

Previous studies have suggested that FoxO proteins can regulate the expression of IR [27] and IRS-2 [28]. We found that IR and IRS-1 mRNA levels were unchanged in TA muscle tissue samples from male TKO and control mice (Supp. Fig. S2E). Interestingly, IRS-2 mRNA levels were markedly decreased in muscle tissue samples from TKO compared to control in both males and females (Supp. Figs. S2E–S2F), indicating a conserved regulation of IRS-2 expression by FoxOs in muscle. Female mice also showed a mild decrease in IR mRNA levels but did not show any differences in IRS-1 mRNA (Supp Fig. 2F). The changes in insulin signaling in male TKO muscle were specific to the PI3K-AKT pathway as no differences in p-ERK1/2 were observed between insulin-stimulated TKO and control muscle tissue samples from male or female mice (Supp. Figs. S2G–S2J).

In assessing insulin signaling proteins, we observed that the western blot for total AKT in male FoxO-TKO muscle showed two bands (Figure 2A) and total AKT tended to decrease (Supp. Fig. S2B). To gain insight into the sex-specific signaling defects that occur in FoxO-TKO mice, we investigated AKT isoform expression in TA muscle from male and female mice, relative to littermate controls. AKT1 levels were unchanged in either sex, relative to controls (Figure 2G–H, J–K). Interestingly, total AKT2 levels were significantly decreased in males (Figure 2H). This is relevant because AKT2 controls the metabolic effects mediated by AKT isoforms, demonstrated by the fact that $AKT2^{-/-}$ mice display hyperglycemia and features of metabolic syndrome, while $AKT1^{-/-}$ mice do not [29,30]. $AKT2^{-/-}$ mice show reduced insulin-stimulated glucose uptake in EDL [29], and AKT2 mediates the improvement in muscle glucose uptake after caloric restriction [31]. Quantitative RT-PCR of the two isoforms also showed that mRNA levels of AKT2 were decreased in the TAs from male FoxO-TKO, compared to controls (Figure 2I). This indicated that the expression of AKT2 in muscle depended on FoxOs in males. However, females showed no differences in AKT2 protein or mRNA levels relative to their littermate controls (Figure 2J–L). Thus, insulin signaling in FoxO-TKO mice showed divergent effects based on sex. Male FoxO-TKO mice show diminished signaling to AKT associated with decreased AKT2 expression, while female TKO display normal insulin signaling in muscle.

3.3. FoxO deletion decreases glucose uptake, insulin action, and AKT2 expression in glycolytic EDL muscle from male mice, but not oxidative soleus muscle

To determine whether the impairment in insulin signaling in male FoxO-TKO mice leads to a functional consequences, we next measured glucose uptake and insulin signaling in glycolytic EDL and oxidative soleus muscles from both male and female TKO and control mice. In control male mice at 8 weeks of age, glucose uptake was significantly increased in both the EDL and soleus muscles in response to insulin.

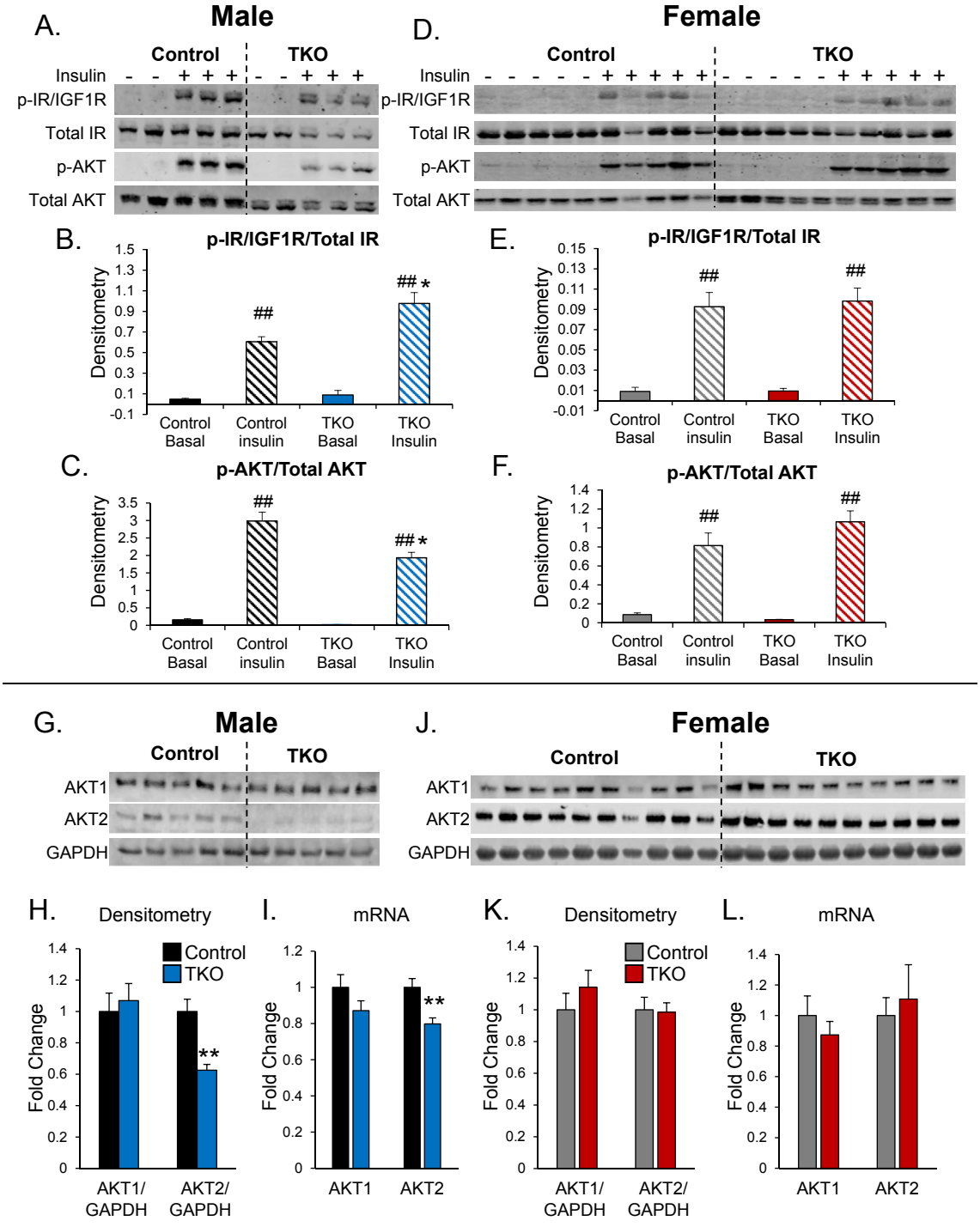

Figure 2: FoxO deletion reveals sex-based differences in muscle insulin signaling and AKT2 expression. FoxO-TKO and littermate controls were injected with either 5U of insulin or saline via the vena cava. Western blot analyses of insulin signaling targets in TA muscle from male (A) control and TKO mice. Densitometry of p-IR/IGF1R normalized to total IR (B) and p-AKT^{S473} (p-AKT) normalized to total AKT (C) from panel A. (n = 2–3 per group for males). Western blot in TA muscle from female (D) control and TKO mice. Densitometry of p-IR/IGF1R normalized to total IR (E) and p-AKT^{S473} normalized to total AKT (F) from panel D. (n = 5 per group for females). Western blot for AKT1 and AKT2 isoforms in TA from male mice (G), and densitometry (H) of panel G (n = 5 per group). Quantitative RT-PCR of AKT1 and AKT2 mRNA in TA from male control and TKO mice (I) (n = 9 per group for males). Western blot for AKT1 and AKT2 isoforms in TA from female mice (J), and densitometry (K) of panel J. Quantitative RT-PCR of AKT1 and AKT2 mRNA in TA from female control and TKO mice (L). (n = 10 per group for females). *p < 0.05, **p < 0.01 TKO vs. control with same treatment; ##p < 0.01 basal vs. insulin in the same genotype; a two-way ANOVA was used for panels A–F, a t-test was used for panels G–L.

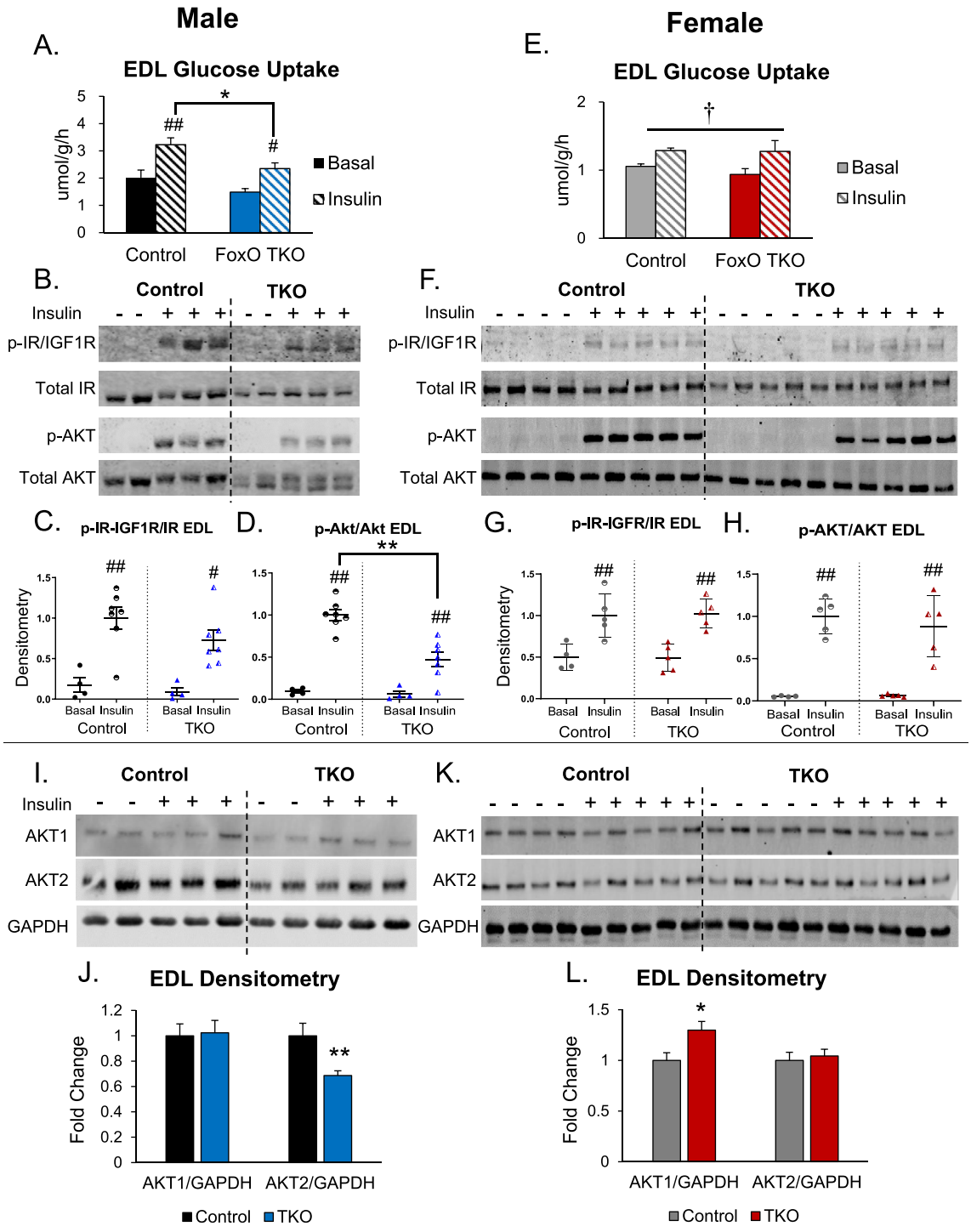

Figure 3: FoxO deletion decreases glucose uptake, insulin action, and AKT2 expression in glycolytic EDL muscle from male mice, but not female. Glucose uptake into isolated EDL muscles from male mice (A) was measured under basal and insulin-stimulated conditions (n = 5–6 per group, aged 8 weeks). Western blot analyses of EDL muscles from male mice injected with either saline or 5U of insulin (B) (n = 4–7 per group). Densitometry from panel B of p-IR/IGF1R normalized to total IR (C) and p-AKT^{S473} normalized to total AKT (D). Glucose uptake into isolated EDL muscles from female mice (E) was measured under basal and insulin-stimulated conditions (n = 8–9 per group for females, aged 15–25 weeks). Western blot analyses of EDL muscles from female mice (F) (n = 5 per group). Densitometry from panel F of p-IR/IGF1R normalized to total IR (G) and p-AKT^{S473} normalized to total AKT (H). Western blot for AKT1 and AKT2 isoforms in EDL from male mice (I), and densitometry (J) of panel I. Western blot for AKT1 and AKT2 isoforms in EDL from female mice (K), and densitometry (L) of panel K. *- $p < 0.05$, **-$p<0.01$ TKO vs. control with same treatment; #$p < 0.05$, ##$p < 0.01$ basal vs. insulin in the same genotype; †-$p<0.05$ insulin main effect by two-way ANOVA. A two-way ANOVA was used for panels A–H, a t-test was used for panels I–L.

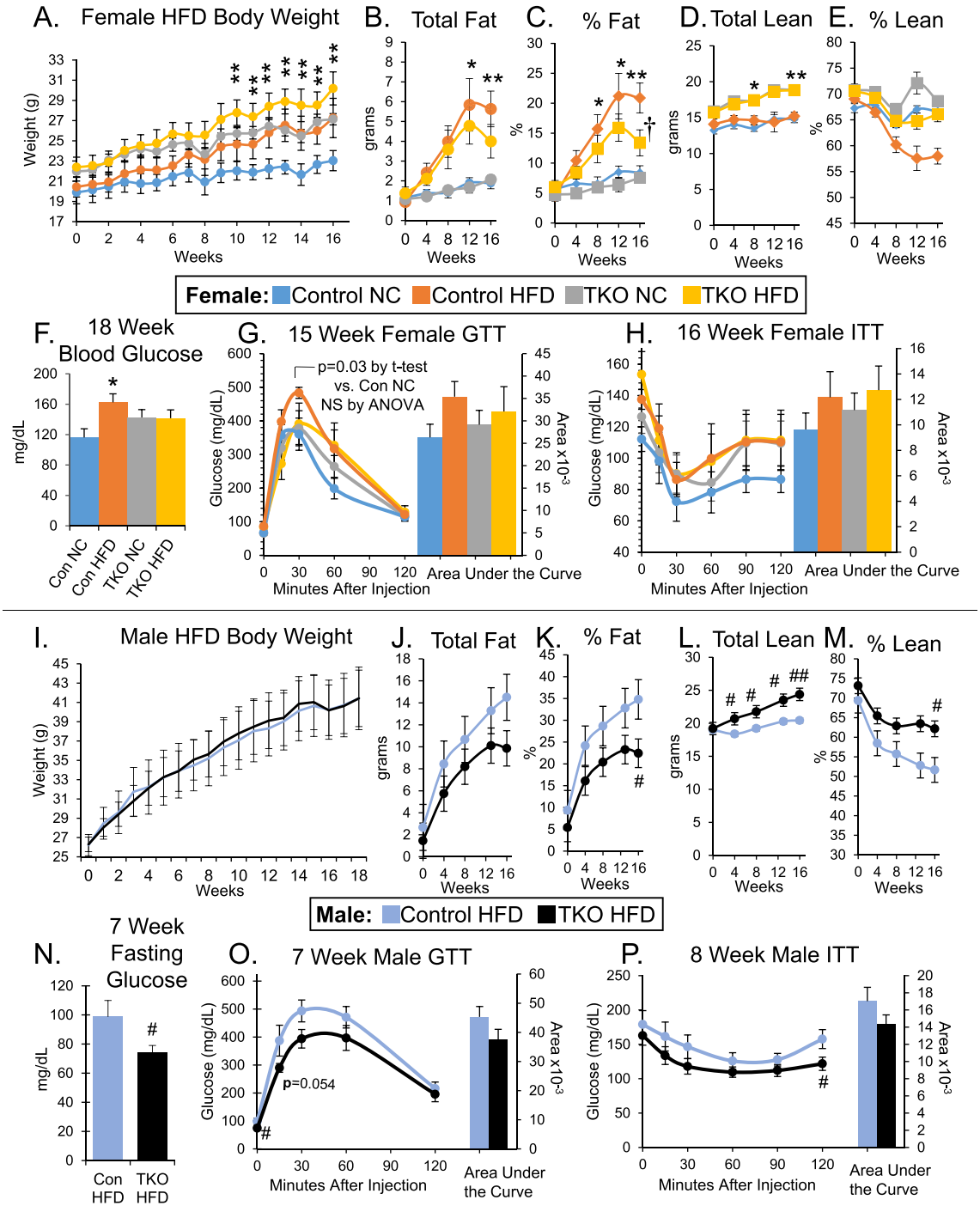

Figure 4: Deletion of FoxOs in muscle mitigates fat gain and metabolic derangements from High Fat Diet. Average body weights from 0–16 weeks (A) in female control and FoxO-TKO mice on normal chow (NC) or high-fat diet (HFD). Body composition measurements of total fat mass (B), % fat (C), total lean mass (D), and % lean (E) during 16 weeks of HFD treatment in female control and TKO mice. Blood glucose levels (F), GTT (G), and ITT (H) after 15–18 weeks on HFD. (n = 6–8 females per group.) Average body weights from 0 to 16 weeks (I) in male control and FoxO-TKO mice on a high-fat diet (HFD). Body composition measurements of total fat mass (J), % fat (K), total lean mass (L), and % lean (M) during 16 weeks of HFD treatment in male control and TKO mice. Fasting blood glucose levels (N), GTT (O), and ITT (P) after 7–8 weeks on HFD. (n = 6–10 males per group.) *-p<0.05, **-p<0.01 compared to Control NC by two-way ANOVA; †-p<0.05 for TKO HFD vs Con HFD by two-way ANOVA; #p < 0.05, ##p < 0.01 compared to male Control HFD by t-test.

However, glucose uptake was decreased in insulin-treated EDL muscle from TKO mice compared to that in insulin-treated controls (Figure 3A). Interestingly, insulin-stimulated glucose uptake in soleus muscles from male TKO mice was unchanged relative to insulin-stimulated soleus from controls (Supp Fig. 3A). In a separate experiment done on 15–25 week-old females, insulin treatment increased glucose uptake equally in control and TKO EDL, (Figure 3E) and soleus muscles (Supp Fig. 3E). Given that TA muscles from male TKO mice showed diminished

insulin-stimulated AKT phosphorylation and decreased AKT2 levels, we determined insulin action and AKT2 levels in the EDL and soleus muscles. In male mice, western blot analyses showed that p-IR/IGF1R normalized to total IR increased in insulin-treated EDL (Figure 3B—C) and soleus (Supp Figs. S3B—S3C) regardless of genotype. Consistent with observations in TA muscle, downstream phosphorylation of AKT was impaired in EDL (Figure 3B,D) and soleus (Supp Figs. S3B and S3D) from male TKOs compared to male controls. However, in females, there were no differences in insulin-stimulated p-IR/IGFR or p-AKT levels in EDL (Figure 3F—H) or soleus (Supp Figs. S3F—S3H) muscles regardless of genotype.

AKT2 expression in males was significantly decreased in EDL muscles from TKO mice compared to controls, with no differences in AKT1 (Figure 3I—J). By contrast, AKT1 and AKT2 levels were unchanged in soleus muscle samples from TKO and control mice (Supp Figs. S3I—S3J). Surprisingly, AKT1 protein levels were increased in female EDL muscle (Figure 3K—L). We did not find any differences in AKT2 expression in females in either the EDL and soleus muscles (Figure 3L, Supp Fig. S3K—S3L). We also determined the levels of Glut4 glucose transporters and TBC1D1 downstream of AKT. Glut4 expression was higher in the soleus compared to the EDL (Supp. Fig. S4A). Glut4 levels tended to be higher in EDL muscles from FoxO TKO mice than from control mice (Supp. Figs. S4A—S4B), but this did not reach statistical significance. Glut4 levels were not different between soleus muscle from TKO and control mice (Supp. Figs. S4A and S4C). AS160 (aka TBC1D4) and TBC1D1 are RabGAP proteins that inhibit Glut4 translocation and glucose uptake in muscle until they are phosphorylated. AS160 is expressed highly in soleus and is relatively insulin-responsive, while TBC1D1 is expressed in EDL and glycolytic muscle and appears to be more exercise responsive [32—34]. In FoxO TKO EDL muscle, TBC1D1 expression tended to increase (Supp. Figs. S4A and S4D). We were unsuccessful performing western blots for p-AS160 (data not shown). These data indicate that the impairment in muscle insulin signaling of male FoxO TKO mice attenuated insulin-stimulated glucose uptake in glycolytic muscles. This is associated with diminished AKT activation and decreased AKT2 expression. Thus, FoxOs control insulin action in glycolytic muscle via regulation of AKT2 expression in a sexually dimorphic manner.

3.4. Deletion of FoxOs in skeletal muscle mitigates weight gain and metabolic derangements from a HFD

To investigate the effects of muscle-specific FoxO deletion on diet-induced obesity and insulin resistance, we fed female and male TKO and control (Con) mice a HFD containing 60% calories from fat starting at 8—10 weeks of age, and continued the diet for a total of 18 weeks (26—28 weeks of age). Female FoxO TKO mice tended to be 10% heavier than control mice (not significant by ANOVA). As expected, Con HFD-fed mice and TKO HFD-fed mice gained more weight than Con NC-fed mice over 16 weeks of dietary intervention (Figure 4A). By the end of 16 weeks, Con HFD-fed mice and TKO HFD-fed mice gained 33% and 34% above baseline weight, respectively. Interestingly, body weight of TKO NC-fed mice was significantly higher than that of Con NC-fed mice (2-way ANOVA, NC:Con vs. NC:TKO, $p = 0.04$), but not significantly different than TKO HFD-fed mice (Supp. Fig. S5A). Body composition measures showed that HFD-fed mice of both genotypes exhibited increased fat mass compared to the NC-fed mice, but the Con HFD-fed mice gained more fat mass than the TKO HFD-fed mice (Figure 4B—C).

Interestingly, lean mass increased by more than 3 g in TKO groups regardless of diet, whereas control groups gained fewer than 2 g over the 16-week diet study (Figure 4D—E). Mild improvements in glucose metabolism accompanied the attenuation of fat gain in the female TKO HFD-fed group. Randomly fed blood glucose levels after 18 weeks of HFD were increased in Con HFD-fed mice, but not in the TKO groups (Figure 4F). Serum triglyceride and glycerol levels showed a similar pattern to glucose levels with a trend toward increased levels in the Con HFD-fed mice, but no differences between the TKO NC-fed and TKO HFD-fed mice (Supp. Fig. S5B). Serum insulin levels also tended to increase in Con HFD-fed mice and in both TKO groups, but with enough variability that no significant differences were observed (Supp. Fig. S5C). After 7 weeks on the HFD, female Con and TKO mice showed glucose intolerance relative to NC groups (Supp. Fig. S5D). Interestingly glucose excursion during an ITT tended to be higher in control HFD-fed, TKO NC-fed, and TKO HFD-fed mice (Supp. Fig. S5E) but did not reach statistical significance. After 15 weeks of HFD, female Con mice remained mildly glucose intolerant (Figure 4G). However, TKO HFD-fed mice showed glucose excursions and AUC values that were indistinguishable from TKO NC-fed mice. Similarly, Con HFD-fed mice tended to have higher glucose levels during the ITT, suggesting decreased insulin sensitivity, although these did not reach statistical significance (Figure 4H). Again, glucose excursions during ITT of the TKO mice on NC or HFD were indistinguishable (Figure 4H).

We hypothesized that the impaired insulin action in muscle from male FoxO TKO mice would exacerbate metabolic derangements from diet-induced obesity. Male Con and TKO mice showed no differences in weight gain on HFD (Figure 4I). However, body composition again showed attenuated fat gain by 16 weeks in male TKO mice compared to male Cons (Figure 4J—K) and increased lean mass in TKO mice (Figure 4L—M). By 7—8 weeks of HFD, fasting glucose levels were lower in TKO HFD-fed male mice relative to controls (Figure 4N), and glucose tolerance tended to improve (Figure 4O). Insulin tolerance was mildly improved in TKO HFD-fed mice relative to control HFD-fed mice (Figure 4P). By 16—17 weeks of HFD, differences in GTT and ITT excursions in male TKO HFD-fed and Con HFD-fed mice were no longer statistically significant (Supp. Figure 5F—G). These data show that deletion of FoxOs in muscle induces muscle hypertrophy in both male and female mice, mitigates fat gain on a HFD, and mildly attenuates glucose abnormalities from diet-induced obesity.

3.5. Metabolic analysis demonstrates increased energy expenditure and activity in FoxO-TKO mice relative to controls

To determine the metabolic factors that contribute to the protection from fat gain in FoxO-TKO mice, we performed indirect calorimetry on control and FoxO-TKO mice during week 14 of NC and HFD treatment (age 22—24 weeks old) using the Promethion home cage system. For female cohorts, we designed the experiment to monitor the mice for 48 h of *ad libitum* access to their respective diets (Fed), followed by 24 h of fasting (Fast) and 24 h of refeeding (refeed) (Figure 5A). During the fed cycle, energy expenditure (EE) was increased in TKO mice compared to control mice regardless of diet ($p < 0.001$ genotype main effect by ANOVA) (Figure 5A—B). During the fasting and refeeding periods, these differences in EE were diminished to the point that the four groups were no longer significantly different during the 24 h of refeeding (Figure 5B).

We reasoned that the increase in muscle mass in female TKO mice would contribute to increased energy expenditures. When normalized to lean body mass, EE in the TKO groups was similar to controls for both the NC-fed and HFD-fed mice (Figure 5C) indicating that increased lean mass contributed to increased EE in female TKO mice. VO_2 and VCO_2 were also increased in TKO NC-fed and TKO HFD-fed mice relative to Con NC-fed mice during the fed period (Supp. Figs. S6A—S6B), and these effects were again proportional to

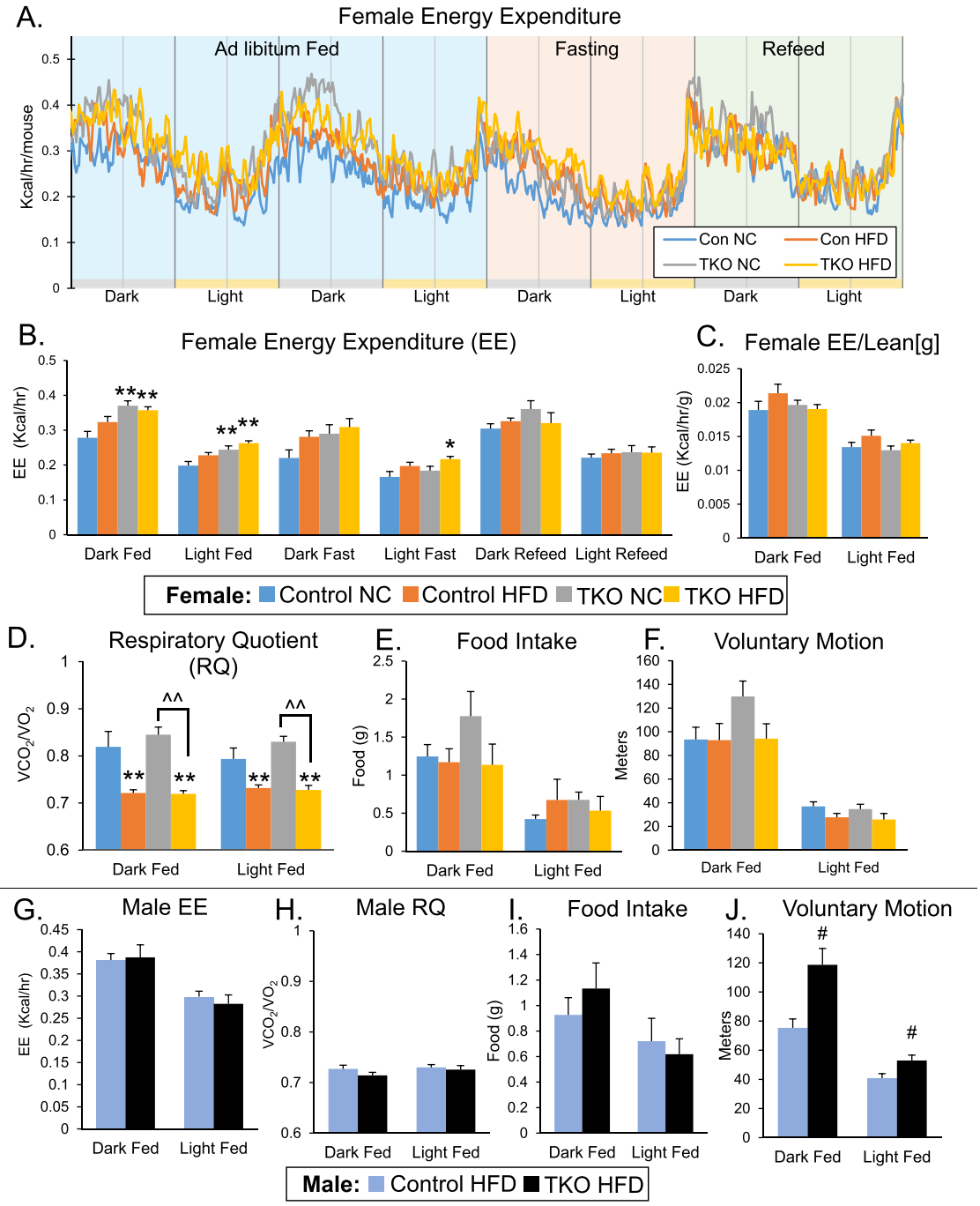

Figure 5: The metabolic analysis demonstrates increased energy expenditure and activity in FoxO-TKO mice relative to controls. Energy expenditure (EE) measured in female mice by indirect calorimetry (A) over 48 h of standard feeding followed by 24 h of fasting and 24 h of refeeding (30-hour acclimation period was done before displayed measurements). Average energy expenditure (B) per mouse for dark and light cycles during the Fed/Fasting/Refeeding experiment in panel A. Average energy expenditure normalized to lean body mass (C) for the *ad libitum* fed cycles. Respiratory quotient (D), food intake (E), and voluntary motion (F) of female control and TKO mice during dark fed and light fed cycles of the indirect calorimetry experiment. (n = 6–8 females per group). Energy expenditure (G), respiratory quotient (H), food intake (I), and voluntary motion (J) of male control and TKO mice on HFD during dark fed and light fed cycles. (n = 6 control and 10 TKO males per group). *-p<0.05, **-p<0.01 compared to Control NC by two-way ANOVA; ^-p<0.01 TKO HFD vs TKO NC by two-way ANOVA; #p < 0.05 compared to male Control HFD by t-test.

increased lean mass in the TKO mice (Supp Figs. S6C–S6D). Respiratory quotient (RQ) values showed that HFD treatment in Con HFD-fed and TKO HFD-fed mice appropriately lowered RQ to around 0.72 (Figure 5D).

Interestingly, TKO mice on NC show an appropriate decrease in RQ during fasting and increase with re-feeding, similar to the Con NC-fed mice (Supp. Fig. S6E). Food intake, measured in grams, was unchanged between the experimental groups (Figure 5E), although TKO NC-fed mice did tend to eat more than the other groups and drank significantly more water during the dark fed period (Supp Fig. S6F). Of note, the caloric density of the HFD was 68% higher than NC (see Methods 2.3), so the HFD-fed controls and HFD-fed TKOs consumed

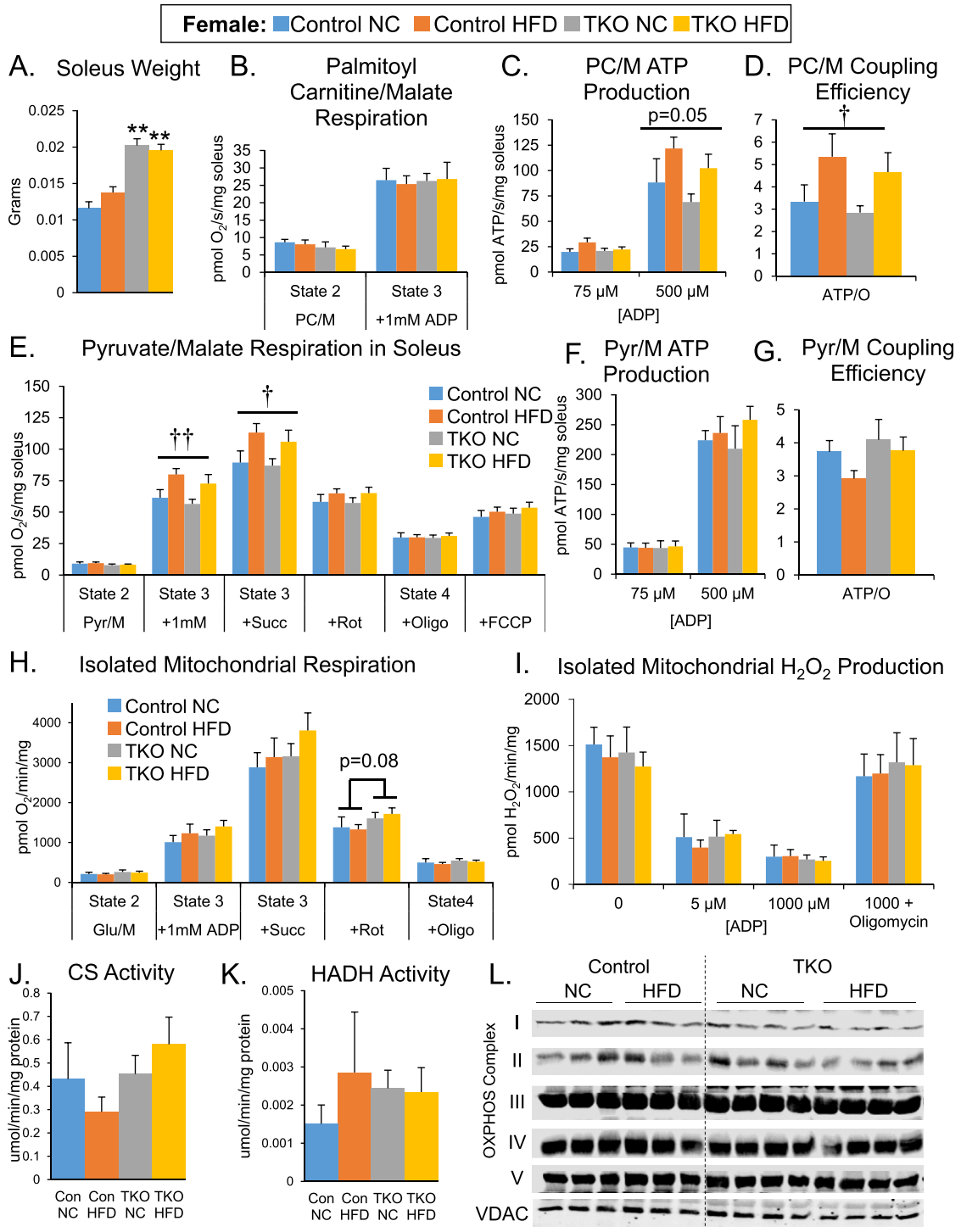

Figure 6: Muscle mass is increased, and mitochondrial function is maintained in FoxO-TKO mice. Soleus weight (A) in female control and TKO mice on normal chow or HFD. Basal (state 2) and maximal (state 3) respiration in soleus muscle permeabilized fibers with Palmitoyl carnitine (PC)/Malate(M) substrates (B). ATP production rates in soleus fibers with PC/M substrates (C) at sub-maximal (75 µM) and maximal (500 µM) ADP concentrations. Ratio of ATP produced per oxygen consumed (D) by soleus fibers in panels B and C. Basal and maximal respiration in soleus permeabilized muscle fibers with Pyruvate (Pyr)/Malate(M) substrates, then sequential addition of succinate (Succ), rotenone (Rot), oligomycin (oligo), and FCCP (E). ATP production rates (F) and ATP/O ratio (G) with Pyr/M substrates. Basal and maximal respiration in isolated mitochondria from mixed gastrocnemius/quadriceps using Glutamate (Glu)/Malate(M) substrates, then sequential addition of succinate, rotenone, and oligomycin (H). Mitochondrial H_2O_2 production from isolated mitochondria (I) in the presence of Glutamate/Malate/Succinate substrates, with the addition of sub-maximal (5 µM) and maximal (1000 µM) ADP concentrations, and/or oligomycin. Citrate synthase (J) and hydroxy-acyl-CoA dehydrogenase (HADH) (K) enzyme activity measured in quadriceps muscle tissue lysates from female TKO and control mice. OXPHOS subunits measured by western blot in TA muscle tissue lysates from female TKO and control mice fed NC or HFD for 18 weeks (L). ($n = 6–8$ per group) **-$p<0.01$ compared to Control NC-fed mice by two-way ANOVA; †$p < 0.05$, ††$p < 0.01$ diet main effect by two-way ANOVA (HFD groups as a whole were different from NC groups, but individual dietary/genotype groups were not statistically different).

more calories than the respective NC-fed groups. In females, the changes in EE were not accounted for by activity, as no changes were seen in voluntary motion in all groups (Figure 5F). Still-motion time, or the time that the animals are not moving, eating, drinking, or grooming, was significantly higher in HFD treated mice, regardless of genotype, and was lowest in TKO NC-fed mice during the dark fed period (Supp. Fig. S6G).

Indirect calorimetry was also performed on male TKO and control mice on HFD during 48 h of *ad libitum* feeding. Interestingly, EE was unchanged in male TKO HFD-fed mice compared to control HFD-fed mice (Figure 5G) but was reduced when normalized to lean mass (Supp. Fig. 6I). VO_2 and VCO_2 were also unchanged in male TKO HFD-fed mice relative to Con HFD-fed mice (Supp. Figs. S6J—S6K). RQ was again suppressed in both Con HFD-fed and TKO HFD-fed male mice (Figure 5H), and food intake was not different between the experimental groups (Figure 5I). In contrast to female mice, male TKO mice on HFD were significantly more active than male controls (Figure 5J). These data indicate that sex-based differences in metabolism contribute to the protection from gain of fat mass in TKO HFD-fed mice. In female TKO mice, increases in EE that were proportional to increases in lean mass dominated; whereas, increased activity in male TKO mice, relative to control HFD-fed mice, was associated with improved metabolic health.

3.6. Muscle mass is increased, and mitochondrial function is maintained in FoxO-TKO mice

Enhanced muscle mitochondrial function has been associated with improved metabolic homeostasis. Conversely, obesity and diabetes have been associated with muscle mitochondrial dysfunction in some [17,35], but not all cases [20]. We measured mitochondrial function in both saponin-permeabilized soleus fibers and isolated mitochondria from female control and TKO mice fed NC or HFD for 18 weeks. Soleus muscles from TKO NC-fed and TKO HFD-fed mice were ~80% larger than control groups (Figure 6A). Maximal respiratory capacity using a fat-derived substrate, palmitoyl-carnitine/malate, did not differ among the four groups (Figure 6B). However, ATP production rates trended higher in soleus muscles from both the Con HFD-fed and TKO HFD-fed groups and coupling efficiency was increased in these groups (Figure 6C—D). Skeletal muscle primarily relies on glycolysis and glucose oxidation (a.k.a. pyruvate utilization) in mitochondria for energy production. Interestingly, maximal respiratory capacity in soleus fibers was increased after HFD feeding in both Con and TKO groups using pyruvate/malate (Pyr/M) as substrates (Figure 6E). Upon addition of succinate, a complex II substrate, respiration remained higher in HFD-fed groups regardless of genotype, but these increases were lost upon sequential addition of rotenone (a complex I inhibitor), oligomycin (a complex V inhibitor), and FCCP (an uncoupler). No differences were seen in ATP production rates with Pyr/M or the ATP/O ratio (Figure 6F—G). It is important to note that these measurements are normalized to muscle mass that is increased in TKO groups, indicating that mitochondrial metabolism is maintained even in the hypertrophic state of FoxO-TKO mice.

Mitochondrial respiration using isolated mitochondria from combined Quad/Gastroc muscles also showed no change in O_2 flux in any of the groups with glutamate/malate although respiration trended higher with succinate/rotenone when comparing TKO mitochondria to controls regardless of diet (Figure 6H). Diabetes has been associated with increased reactive oxygen species (ROS) generation, but we observed no difference in H_2O_2 production rates across a range of ADP concentrations in isolated mitochondria from control and TKO mice regardless of diet (Figure 6I). In agreement with the mitochondrial function, there was no change in citrate synthase activity or HADH activity among the groups (Figure 6J—K). Interestingly, a subunit of complex I of the electron transport chain (ETC) was reduced in TKO mice (Figure 6L and Supp. Fig. S6H), but other ETC subunits were unchanged. In males, we assessed mitochondrial enzyme activities and saw no differences in CS or HADH activity in quadriceps homogenate from male Con HFD and TKO HFD (Supp. Fig. S6L—S6M). These data show that mitochondrial function normalized to muscle mass is maintained in female FoxO-TKO mice, even in the presence of muscle hypertrophy and likely contributes to the increased energy expenditure.

3.7. Muscle-specific FoxO deletion prevents triglyceride accumulation in muscle but minimally changes inflammatory markers in the liver

Diet-induced obesity is associated with lipid accumulation in non-adipose tissue and inflammation in liver. As expected, HFD feeding led to a 2.7-fold increase in triglycerides in Quad muscle from female control mice, but this increase was prevented in female TKO HFD (Figure 7A). Male TKO HFD-fed mice showed decreased triglyceride in Quad muscle compared to male Control HFD (Figure 7B). Hematoxylin and eosin (H&E) staining of liver samples from female mice appeared to show decreased steatosis (Figure 7C), but quantification of liver triglyceride content showed increased triglycerides in Con HFD-fed and TKO HFD-fed groups compared to NC-fed groups (Figure 7D), with no change between HFD-fed groups. Absolute liver weights were increased in female TKO HFD-fed mice compared to Con NC-fed mice (Figure 7E) but were significantly decreased, when normalized to body weight (Figure 7F). Inflammatory markers in liver measured by quantitative RT-PCR showed minimal changes other than a dietary main effect for increased macrophage marker, F4/80, in HFD groups (Figure 7G). Similarly, in males, there were no differences in liver triglycerides, liver weights, or inflammatory markers in the liver between male TKO HFD-fed and Con HFD-fed mice (Figure 7H—K). These data indicate that deletion of FoxOs in muscle is associated with reduced triglyceride accumulation in muscle after HFD, but minimal changes in metabolic or inflammatory abnormalities in the liver.

3.8. Muscle-specific FoxO deletion attenuates fat gain after HFD but does not alter adipose inflammation, brown markers in iWAT or adipokine expression

Diet-induced obesity is associated with increased adipose tissue inflammation and alterations of circulating adipokines. Adipose tissue weights increased in females on a HFD, regardless of diet (Supp. Fig. S7A). When normalized to body weight, peri-gonadal (pg) and inguinal (i) white adipose tissue (WAT) increased in both female HFD-fed groups, but iWAT/BW in TKO HFD-fed mice increased less such that TKO HFD-fed mice were not different from Con NC-fed mice (Figure 8A), which agrees with the body composition data in Figure 4C. Inflammatory markers in female pgWAT were largely unchanged, other than the increased macrophage marker CD11b in the HFD-fed groups (Figure 8B). Browning of iWAT is often associated with increased energy expenditure, but we saw no difference in brown adipose tissue (BAT) markers in female TKO iWAT compared to control iWAT regardless of diet (Figure 8C), or in BAT weights and BAT gene expression (Supp. Figs. S7B—S7C). Expression of adiponectin mRNA and leptin mRNA in iWAT was variable, but not significantly changed in female TKO mice and control iWAT, regardless of diet (Figure 8D—E). In male TKO HFD-fed mice, pgWAT weights tended to decrease (Supp. Fig. S7D) and were significantly lower than male Con HFD-fed mice when normalized to body weight (Figure 8F). This is important because

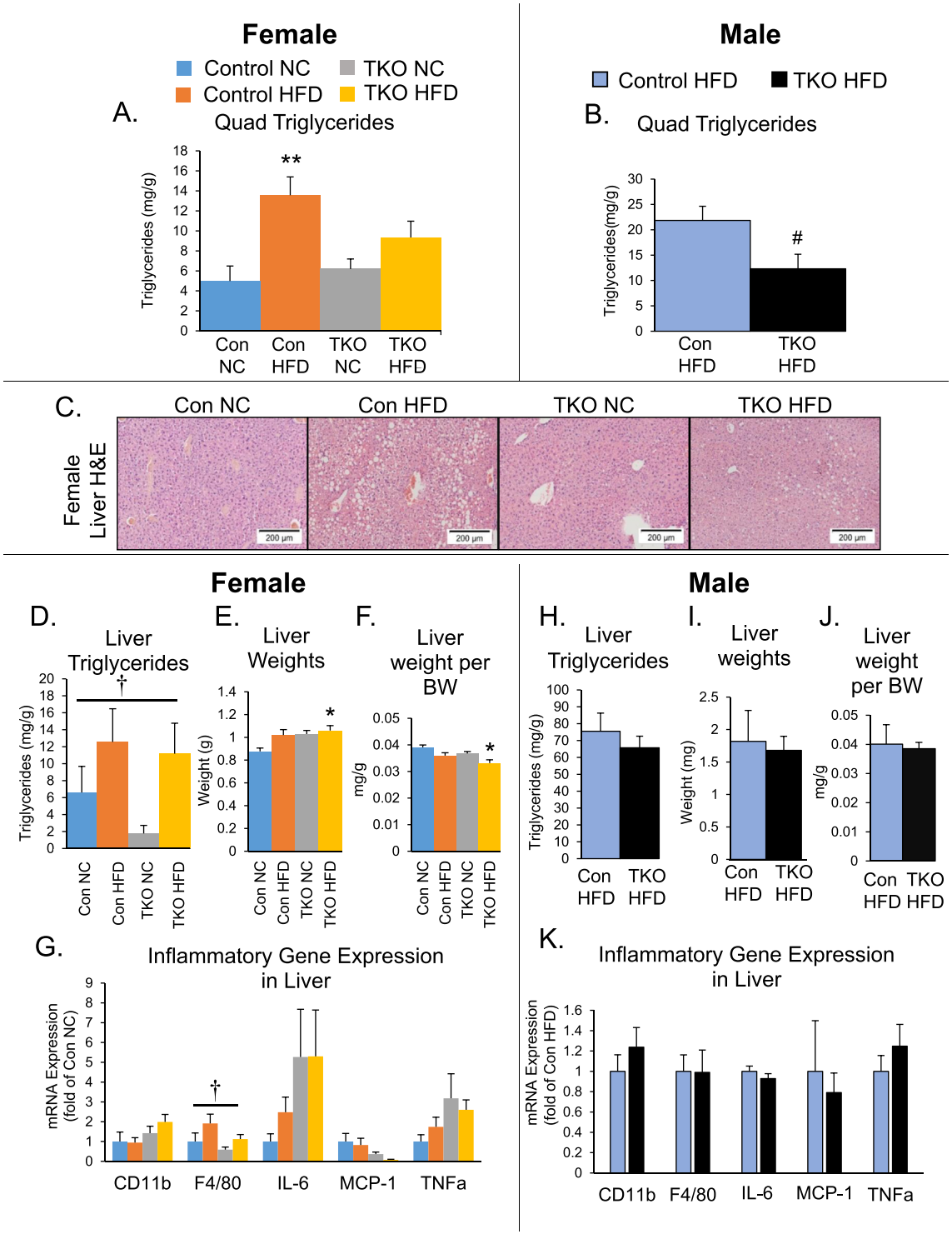

Figure 7: Muscle-specific FoxO deletion attenuates muscle triglyceride accumulation after HFD feeding but does not alter liver inflammation. Quadriceps (Quad) triglyceride content from female (A) and male (B) control and FoxO-TKO mice on HFD for 18 weeks. Representative images of liver tissue from female control and TKO mice on NC or HFD stained with Hematoxylin and Eosin (C). Liver triglycerides (D), liver weights (E), liver weight per body weight (F), and inflammatory markers measured by quantitative RT-PCR (G) in the liver from female mice. Liver triglycerides (H), liver weights (I), liver weight per body weight (J), and inflammatory markers in the liver from male mice (K). *-$p<0.05$, **-$p<0.01$ compared to Control NC-fed mice by two-way ANOVA; †$p < 0.05$, diet main effect by two-way ANOVA. #$p < 0.05$ compared to male Control HFD by t-test.

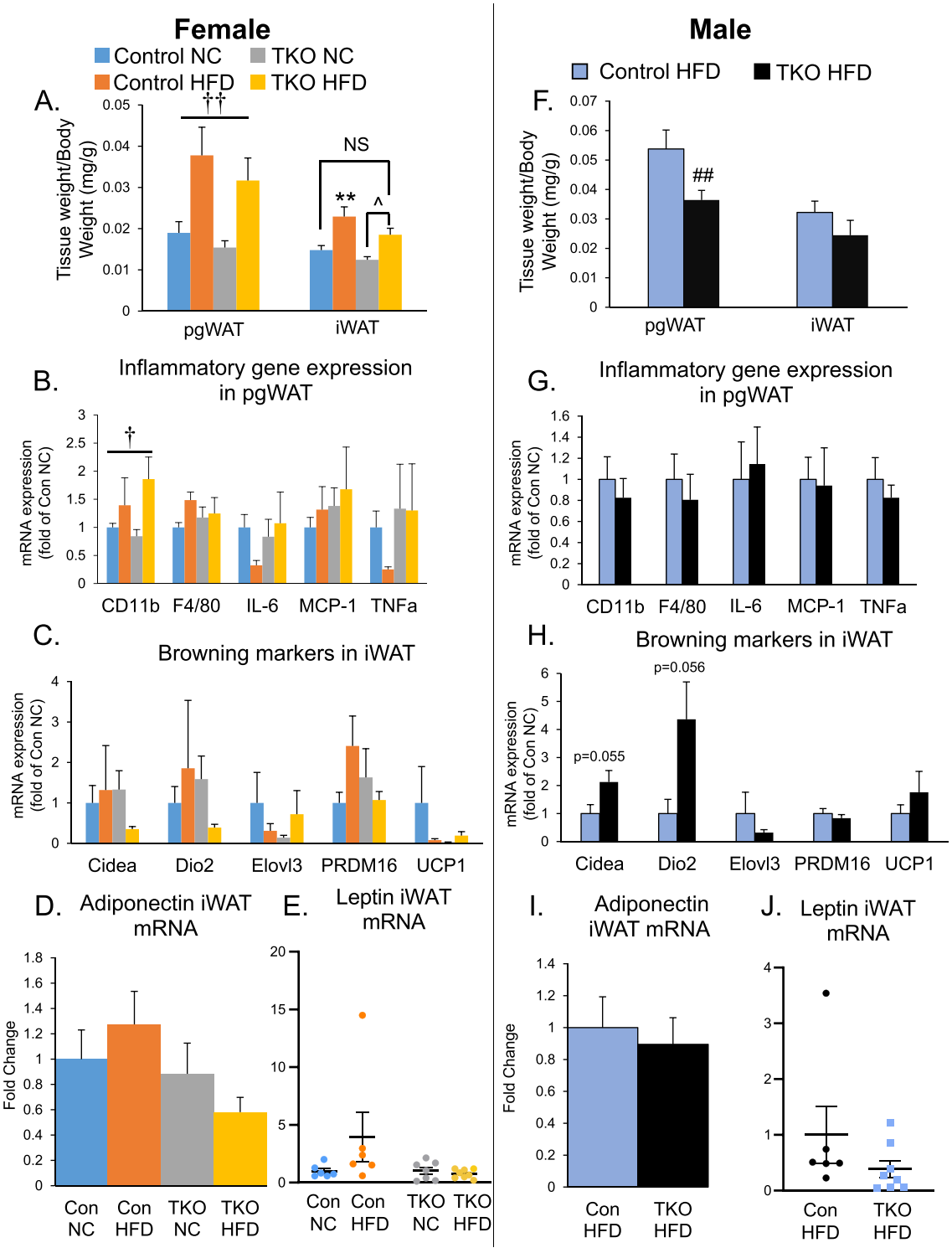

Figure 8: Muscle-specific FoxO deletion attenuates fat gain after HFD feeding but does not alter adipose inflammation, brown markers in iWAT or adipokine expression. Adipose tissue weights (A) for perigonadal WAT (pgWAT) and inguinal white adipose tissue (iWAT) normalized to body weight from female mice. Quantitative RT-PCR performed on female pgWAT for inflammatory markers (B). Quantitative RT-PCR performed on female iWAT for browning markers (C) and adipokines (D–E). Adipose tissue weights (F) for pgWAT and iWAT normalized to body weight from male mice. Quantitative RT-PCR performed on male pgWAT for inflammatory markers (G). Quantitative RT-PCR performed on male iWAT for browning markers (H) and adipokines (I–J). NS-not significant. †$p < 0.05$, ††$p < 0.01$, diet main effect by two-way ANOVA; **-$p<0.01$ compared to Control NC-fed mice by two-way ANOVA; ^-$p<0.05$ TKO HFD vs. TKO NC by two-way ANOVA; ##$p < 0.01$ compared to male Control HFD by t-test.

there were no differences in absolute body weight at the end of the study (Figure 4I). Again, inflammatory markers in pgWAT were unchanged between male HFD-fed groups (Figure 8G). The BAT markers Cidea and Dio2 tended to increase in male TKO iWAT (Figure 8H), but other BAT markers in iWAT, adiponectin in iWAT, leptin in iWAT (Figure 8H–J), and BAT weights and gene expression remained unchanged (Supp. Figs. S7E–S7F). AgRP and POMC neurons in the hypothalamus can regulate energy expenditures, and we observed increased energy expenditures in female TKO mice on both NC and HFD. We measured NPY, AgRP, and POMC expression in the hypothalamus from separate cohorts of female and male TKO mice, but again saw no differences (Supp. Figs. S7G–S7H). These data indicate that the metabolic improvements seen in TKO HFD-fed mice were associated with muscle hypertrophy and reduced adipose tissue mass. Minimal changes were observed in inflammatory markers, browning of WAT, or circulating adipokines.

4. DISCUSSION

Obesity-related complications, including type 2 diabetes and insulin resistance, are major contributors to poor health. There are significant differences in insulin sensitivity between males and females, and these differences may lead to differences in sex-specific rates of prediabetes and diabetes [1,2]. Several human studies have shown that females are more insulin sensitive than males when compared using the hyperinsulinemic-euglycemic clamp technique [4]. Furthermore, females are more glucose tolerant and relatively protected from metabolic derangements due to diet-induced obesity [3]. Skeletal muscle is the primary site for glucose disposal, and muscle insulin resistance can occur decades before the onset of type 2 diabetes [36]. However, the body composition measurements of males and females reveal that females have less lean mass and more fat mass, and females show reduced mitochondrial function in muscle compared to males [37]. Such features are often associated with insulin resistance. Thus, it is imperative to understand the cellular signaling and physiologic mechanisms that underlie muscle growth and insulin sensitivity to develop better therapeutic strategies to treat insulin resistance.

We investigated the role of FoxOs in sex-based differences in muscle growth and glucose homeostasis. Our results reveal that muscle-specific deletion of FoxOs in TKO mice led to ~40% increases in muscle size in both male and female mice. Interestingly, male TKO mice showed impaired insulin action in the muscle that was associated with reduced AKT2 expression, a feature not found in female TKO mice. This insulin resistance in male TKO muscle was functionally important since insulin-stimulated glucose uptake was significantly decreased in glycolytic EDL muscles compared to male controls. This suggests that FoxOs promote insulin sensitivity in males, likely due to increased expression of AKT2.

We also showed that FoxO deletion in muscle mitigated fat gain in both male and female TKO mice compared to their littermate controls. Indirect calorimetry experiments showed that the attenuation of fat gain was due to increased energy expenditure in female TKO mice; in contrast, males showed increased voluntary motion. The decreased fat mass in TKO groups was associated with mild improvements in glucose homeostasis, maintenance of mitochondrial function, and decreased triglyceride accumulation in muscle. Thus, while the loss of FoxOs in muscle from male mice decreased AKT2 to impair insulin action, both males and female TKO mice showed metabolic improvements compared to controls on HFD due to increased muscle mass.

Deletion of FoxOs in muscle led to a specific decrease in AKT2 levels in male mice, but not female mice. The consequence of reduced AKT2 levels in TKO males was impaired insulin action and decreased glucose uptake in glycolytic muscles, similar to previous studies that showed AKT2 is essential for normal glucose uptake in EDL muscle and improvements in muscle glucose uptake after caloric restriction [29,31]. The regulation of AKT2 levels by FoxOs was, at least in part, transcriptionally mediated because AKT2 mRNA levels were also decreased in male TKO mice. Conversely, we have previously published that AKT2 isoforms increased in mice that lacked IR and IGF1R in skeletal muscle [Figs. 2D and S3B in ref [14]], an experimental model with increased FoxO activation [12]. While FoxO deletion in TKO mice was associated with decreased IR protein levels and IRS-2 mRNA levels in both male and female TKO, this did not correlate with insulin-stimulated AKT phosphorylation or with glucose uptake.

AKT2 expression was the one factor associated with the decreased glucose uptake; namely, AKT2 was decreased in male TKO muscles relative to male controls, but there was no difference between female TKO and controls. These data indicate that, in male mice, FoxOs controls insulin action in muscle by regulating AKT2 expression. This reveals an interesting feedback loop whereby fasting decreases insulin levels, leading to increased FoxO activation and AKT2 expression. Upon acute insulin-stimulated activation of AKT2, FoxOs are excluded from the nucleus, thereby decreasing AKT2 mRNA expression and providing feedback inhibition on the signaling cascade.

Previous studies have shown that, under high fat-fed conditions, male mice develop more glucose abnormalities than females [3]; however, the mechanisms for these differences are not fully understood. The preservation of glucose homeostasis in females could be due to the sex hormone, estrogen, because females are protected from metabolic syndrome up to menopause. Indeed, post-menopausal females who receive hormone replacement therapy are at a 21% lower risk of new-onset type 2 diabetes as compared with women who do not receive the treatment [38]. This may be in part due to the marked effects that estrogen has on skeletal muscle through its receptor, ERα [39]. Muscle-specific deletion of ERα led to adipose tissue accumulation and insulin resistance, in part due to mitochondrial dysfunction [40]. Another recent study showed that estrogen itself might act to inhibit FoxO1 in the liver, leading to enhanced glucose homeostasis in females [41]. However, we deleted FoxOs in the muscles of female mice and saw preserved insulin signaling. This suggests a protective effect of estrogen that is independent of FoxO proteins.

ERα signaling may be sufficient to maintain AKT2 levels in the absence of FoxOs. Yeast-two hybrid screens found that FoxOs and estrogen receptors can physically interact [42]. We hypothesize that estrogen increases or enhances FoxO-driven AKT2 mRNA expression. In line with this hypothesis, a recent study showed that estrogen replacement in ovariectomized rats increased whole-body insulin sensitivity and insulin-stimulated phosphorylation of AKT2 and AS160 in muscle; however, no changes were observed in the liver [43]. Conversely, FoxOs may interact with androgen signaling as well. Although the exact mechanisms of this regulation are not fully understood, further investigation into FoxO-ERα co-regulation may reveal mechanisms for these sex-based differences in muscle insulin sensitivity.

Muscle hypertrophy influences glucose homeostasis. In humans, resistance and aerobic exercise can improve glycemic control and improve body composition in patients with obesity and diabetes [44,45]. Mouse models of muscle hypertrophy can be generated in various ways. The FoxO TKO model presented in this study caused muscle hypertrophy that was likely due to the chronic suppression of protein degradation pathways [10,13]. The degree of hypertrophy is similar to myostatin knock-out ($Mstn^{-/-}$) or overexpression of a constitutively active AKT [6,7,46]. $Mstn^{-/-}$ mice exposed to HFD show

decreased overall weight gain, improved glucose and insulin tolerance, and maintained lower circulating markers of metabolic health, such as free fatty acids, triglycerides, and leptin [47]. Myostatin knockout can also attenuate genetic obesity. $Mstn^{-/-}$ mice crossed with ob/ob and agouti models showed increased energy expenditure and decreased fat gain [6]. Myostatin is a TGFβ − like molecule that primarily acts through SMAD transcription factors, a pathway distinct from the PI3K-AKT-FoxO cascade, but with some significant crosstalk [48—50]. AKT is a direct upstream inhibitor of FoxOs. Thus, our FoxO TKO model recapitulated some, but not all, aspects of models with myristoylated AKT (myr-AKT) overexpression. Myr-AKT mice showed marked improvement in glucose and insulin tolerance [7], whereas mild improvements were seen in FoxO TKO mice. As an upstream regulator in the insulin signaling cascade, AKT regulated glucose uptake via AS160 and TBC1D1, pathways independent of FoxOs.

In our study, we observed decreased insulin-stimulated glucose uptake in EDL muscle of FoxO TKO mice, whereas myr-AKT overexpression increased gastrocnemius glucose uptake [7]. A recent study which overexpressed dominant negative FoxOs in muscle tissue also showed decreased glucose uptake, despite increased AKT phosphorylation [15]. Thus, loss of FoxO action does not appear to cause Glut4 translocation, whereas myr-AKT does, potentially contributing to the larger effects on glucose homeostasis.

Irrespective of differences in glucose uptake from other models of hypertrophy, diet-induced fat gain was mitigated in FoxO TKO mice, suggesting that muscle hypertrophy from various causes can attenuate diet-induced obesity. We show that FoxO TKO in muscle decreases fat mass in mice fed HFD with no changes in overall weight, liver inflammation, liver steatosis, adipose inflammation, markers of brown fat, or adipokine expression compared to controls on HFD. However, deletion of FoxOs still led to mild protection from the metabolic consequences of obesity, similar to other models of muscle hypertrophy [6,7]. To investigate this in more depth, we performed mitochondrial bioenergetic assays on soleus muscles from TKO and control mice. Even when normalized to the increased muscle mass, we observed that mitochondrial function was preserved in FoxO TKO mice. This likely contributed to the increased energy expenditure in females. Interestingly, our study did not show a difference in mitochondrial function in muscle from control mice on HFD compared to NC. Indeed, pyruvate respiration in state 3 was actually increased in HFD-treated mice, irrespective of genotype. This is in contrast to some studies on male C57Bl6 mice which showed decreased mitochondrial function after 16 weeks on a HFD [17].

Other studies have not consistently shown mitochondrial dysfunction in response to an HFD [20]. Mouse strain and environmental factors, like gut microbiome, can have marked effects on metabolism [51], and some of these effects can be related to exposure and institution. Nonetheless, we showed that deletion of FoxOs in muscle coordinately increased muscle size and mitochondrial function, which increased energy expenditure in females exposed to HFD.

In summary, sex and body composition are critical regulators of muscle insulin sensitivity; however, the means by which these features mediate changes in insulin action are poorly understood. Our study demonstrates that FoxOs contributes to sexually dimorphic differences in insulin action, at least in part, by promoting the expression of AKT2 in muscle from male mice. Despite the sex-based differences in AKT2 expression, FoxO deletion leads to equivalent muscle hypertrophy in males and females, which mitigates fat gain and glycemic abnormalities when exposed to diet-induced obesity. These results indicate that suppression of FoxO action in muscle may be an important therapeutic goal that could bypass muscle insulin resistance and improve metabolic complications of obesity.

AUTHOR CONTRIBUTIONS

C.M.P. and P.A.S.B. designed the study, researched data, and wrote the manuscript. G.B., J.J., T.L.J., and K.P. researched data, helped design experiments and helped write the manuscript. M.F.H. and L.J.G. researched data and helped design the experiments. B.T.O. designed the study and helped write the manuscript.

ACKNOWLEDGMENTS

This work was supported by NIH grants (K08DK100543) and (R03DK112003) to B.T.O., (R01DK101043) to L.J.G., the Joslin Diabetes Center DRC (P30 DK36836), and the University of Iowa core facility. The authors would like to acknowledge use of the Fraternal Order of Eagle Diabetes Research Center Metabolic Phenotyping Core, the University of Iowa Central Microscopy Research Facility, a core resource supported by the University of Iowa Vice President for Research, and the Carver College of Medicine. Quantitative RT-PCR data was obtained at the Genomics Division of the Iowa Institute of Human Genetics which is supported, in part, by the University of Iowa Carver College of Medicine. We thank Dr. C. Ronald Kahn for his support in facilitating collaboration between Dr. O'Neill and Dr. Goodyear. Brian T. O'Neill is the guarantor of this work and, as such, had full access to all the data in the study and takes responsibility for the integrity of the data and the accuracy of the data analysis.

CONFLICT OF INTEREST

None declared.

APPENDIX A. SUPPLEMENTARY DATA

Supplementary data to this article can be found online at https://doi.org/10.1016/j.molmet.2019.10.001.

REFERENCES

[1] Cowie, C.C., Casagrande, S.S., Geiss, L.S., 2018. Chapter 3: prevalence and incidence of type 2 diabetes and prediabetes. Diabetes in America, NIH Pub No. 12—1468. Bethesda, MD: National Institutes of Health.

[2] Yang, W., Lu, J., Weng, J., Jia, W., Ji, L., Xiao, J., et al., 2010. Prevalence of diabetes among men and women in China. New England Journal of Medicine 362(12):1090—1101.

[3] Pettersson, U.S., Walden, T.B., Carlsson, P.O., Jansson, L., Phillipson, M., 2012. Female mice are protected against high-fat diet induced metabolic syndrome and increase the regulatory T cell population in adipose tissue. PLoS One 7(9):e46057.

[4] Lundsgaard, A.M., Kiens, B., 2014. Gender differences in skeletal muscle substrate metabolism - molecular mechanisms and insulin sensitivity. Frontiers in Endocrinology 5:195.

[5] Haizlip, K.M., Harrison, B.C., Leinwand, L.A., 2015. Sex-based differences in skeletal muscle kinetics and fiber-type composition. Physiology (Bethesda) 30(1):30—39.

[6] McPherron, A.C., Lee, S.J., 2002. Suppression of body fat accumulation in myostatin-deficient mice. Journal of Clinical Investigation 109(5):595—601.

[7] Izumiya, Y., Hopkins, T., Morris, C., Sato, K., Zeng, L., Viereck, J., et al., 2008. Fast/Glycolytic muscle fiber growth reduces fat mass and improves metabolic parameters in obese mice. Cell Metabolism 7(2):159—172.

[8] Eijkelenboom, A., Burgering, B.M., 2013. FOXOs: signalling integrators for homeostasis maintenance. Nature Reviews Molecular Cell Biology 14(2):83–97.
[9] Mammucari, C., Milan, G., Romanello, V., Masiero, E., Rudolf, R., Del, P.P., et al., 2007. FoxO3 controls autophagy in skeletal muscle in vivo. Cell Metabolism 6(6):458–471.
[10] Milan, G., Romanello, V., Pescatore, F., Armani, A., Paik, J.H., Frasson, L., et al., 2015. Regulation of autophagy and the ubiquitin-proteasome system by the FoxO transcriptional network during muscle atrophy. Nature Communications 6:6670.
[11] Sandri, M., Sandri, C., Gilbert, A., Skurk, C., Calabria, E., Picard, A., et al., 2004. Foxo transcription factors induce the atrophy-related ubiquitin ligase atrogin-1 and cause skeletal muscle atrophy. Cell 117(3):399–412.
[12] O'Neill, B.T., Lee, K.Y., Klaus, K., Softic, S., Krumpoch, M.T., Fentz, J., et al., 2016. Insulin and IGF-1 receptors regulate FoxO-mediated signaling in muscle proteostasis. Journal of Clinical Investigation 126(9):3433–3446.
[13] O'Neill, B.T., Bhardwaj, G., Penniman, C.M., Krumpoch, M.T., Suarez Beltran, P.A., Klaus, K., et al., 2019. FoxO transcription factors are critical regulators of diabetes–related muscle atrophy. Diabetes 68(3):556–570.
[14] O'Neill, B.T., Lauritzen, H.P., Hirshman, M.F., Smyth, G., Goodyear, L.J., Kahn, C.R., 2015. Differential role of insulin/IGF-1 receptor signaling in muscle growth and glucose homeostasis. Cell Reports 11(8):1220–1235.
[15] Lundell, L.S., Massart, J., Altintas, A., Krook, A., Zierath, J.R., 2019. Regulation of glucose uptake and inflammation markers by FOXO1 and FOXO3 in skeletal muscle. Molecular Metabolism 20:79–88.
[16] Ruegsegger, G.N., Creo, A.L., Cortes, T.M., Dasari, S., Nair, K.S., 2018. Altered mitochondrial function in insulin-deficient and insulin-resistant states. Journal of Clinical Investigation 128(9):3671–3681.
[17] Bonnard, C., Durand, A., Peyrol, S., Chanseaume, E., Chauvin, M.A., Morio, B., et al., 2008. Mitochondrial dysfunction results from oxidative stress in the skeletal muscle of diet-induced insulin-resistant mice. Journal of Clinical Investigation 118(2):789–800.
[18] Asmann, Y.W., Stump, C.S., Short, K.R., Coenen-Schimke, J.M., Guo, Z., Bigelow, M.L., et al., 2006. Skeletal muscle mitochondrial functions, mitochondrial DNA copy numbers, and gene transcript profiles in type 2 diabetic and nondiabetic subjects at equal levels of low or high insulin and euglycemia. Diabetes 55(12):3309–3319.
[19] Sparks, L.M., Xie, H., Koza, R.A., Mynatt, R., Hulver, M.W., Bray, G.A., et al., 2005. A high-fat diet coordinately downregulates genes required for mitochondrial oxidative phosphorylation in skeletal muscle. Diabetes 54(7):1926–1933.
[20] Franko, A., von Kleist-Retzow, J.C., Bose, M., Sanchez-Lasheras, C., Brodesser, S., Krut, O., et al., 2012. Complete failure of insulin-transmitted signaling, but not obesity-induced insulin resistance, impairs respiratory chain function in muscle. Journal of Molecular Medicine (Berlin) 90(10):1145–1160.
[21] Bruning, J.C., Michael, M.D., Winnay, J.N., Hayashi, T., Horsch, D., Accili, D., et al., 1998. A muscle–specific insulin receptor knockout exhibits features of the metabolic syndrome of NIDDM without altering glucose tolerance. Molecular Cell 2(5):559–569.
[22] Frezza, C., Cipolat, S., Scorrano, L., 2007. Organelle isolation: functional mitochondria from mouse liver, muscle and cultured fibroblasts. Nature Protocols 2(2):287–295.
[23] Lark, D.S., Torres, M.J., Lin, C.T., Ryan, T.E., Anderson, E.J., Neufer, P.D., 2016. Direct real-time quantification of mitochondrial oxidative phosphorylation efficiency in permeabilized skeletal muscle myofibers. American Journal of Physiology - Cell Physiology 311(2):C239–C245.
[24] Yu, L., Fink, B.D., Herlein, J.A., Sivitz, W.I., 2013. Mitochondrial function in diabetes: novel methodology and new insight. Diabetes 62(6):1833–1842.
[25] Spinazzi, M., Casarin, A., Pertegato, V., Salviati, L., Angelini, C., 2012. Assessment of mitochondrial respiratory chain enzymatic activities on tissues and cultured cells. Nature Protocols 7(6):1235–1246.
[26] Boudina, S., Sena, S., O'Neill, B.T., Tathireddy, P., Young, M.E., Abel, E.D., 2005. Reduced mitochondrial oxidative capacity and increased mitochondrial uncoupling impair myocardial energetics in obesity. Circulation 112(17):2686–2695.
[27] Puig, O., Tjian, R., 2005. Transcriptional feedback control of insulin receptor by dFOXO/FOXO1. Genes & Development 19(20):2435–2446.
[28] Zhang, J., Ou, J., Bashmakov, Y., Horton, J.D., Brown, M.S., Goldstein, J.L., 2001. Insulin inhibits transcription of IRS-2 gene in rat liver through an insulin response element (IRE) that resembles IREs of other insulin-repressed genes. Proceedings of the National Academy of Sciences of the United States of America 98(7):3756–3761.
[29] Cho, H., Mu, J., Kim, J.K., Thorvaldsen, J.L., Chu, Q., Crenshaw 3rd, E.B., et al., 2001. Insulin resistance and a diabetes mellitus-like syndrome in mice lacking the protein kinase Akt2 (PKB beta). Science 292(5522):1728–1731.
[30] Cho, H., Thorvaldsen, J.L., Chu, Q., Feng, F., Birnbaum, M.J., 2001. Akt1/PKBalpha is required for normal growth but dispensable for maintenance of glucose homeostasis in mice. Journal of Biological Chemistry 276(42):38349–38352.
[31] McCurdy, C.E., Cartee, G.D., 2005. Akt2 is essential for the full effect of calorie restriction on insulin-stimulated glucose uptake in skeletal muscle. Diabetes 54(5):1349–1356.
[32] Cartee, G.D., 2015. Roles of TBC1D1 and TBC1D4 in insulin- and exercise-stimulated glucose transport of skeletal muscle. Diabetologia 58(1):19–30.
[33] Kramer, H.F., Witczak, C.A., Fujii, N., Jessen, N., Taylor, E.B., Arnolds, D.E., et al., 2006. Distinct signals regulate AS160 phosphorylation in response to insulin, AICAR, and contraction in mouse skeletal muscle. Diabetes 55(7):2067–2076.
[34] Taylor, E.B., An, D., Kramer, H.F., Yu, H., Fujii, N.L., Roeckl, K.S., et al., 2008. Discovery of TBC1D1 as an insulin-, AICAR-, and contraction-stimulated signaling nexus in mouse skeletal muscle. Journal of Biological Chemistry 283(15):9787–9796.
[35] Zabielski, P., Lanza, I.R., Gopala, S., Heppelmann, C.J., Bergen 3rd, H.R., Dasari, S., et al., 2016. Altered skeletal muscle mitochondrial proteome as the basis of disruption of mitochondrial function in diabetic mice. Diabetes 65(3):561–573.
[36] DeFronzo, R.A., Tripathy, D., 2009. Skeletal muscle insulin resistance is the primary defect in type 2 diabetes. Diabetes Care 32(Suppl. 2):S157–S163.
[37] Karakelides, H., Irving, B.A., Short, K.R., O'Brien, P., Nair, K.S., 2010. Age, obesity, and sex effects on insulin sensitivity and skeletal muscle mitochondrial function. Diabetes 59(1):89–97.
[38] Margolis, K.L., Bonds, D.E., Rodabough, R.J., Tinker, L., Phillips, L.S., Allen, C., et al., 2004. Effect of oestrogen plus progestin on the incidence of diabetes in postmenopausal women: results from the Women's Health Initiative Hormone Trial. Diabetologia 47(7):1175–1187.
[39] Hevener, A.L., Zhou, Z., Moore, T.M., Drew, B.G., Ribas, V., 2018. The impact of ERalpha action on muscle metabolism and insulin sensitivity – strong enough for a man, made for a woman. Molecular Metabolism 15:20–34.
[40] Ribas, V., Drew, B.G., Zhou, Z., Phun, J., Kalajian, N.Y., Soleymani, T., et al., 2016. Skeletal muscle action of estrogen receptor alpha is critical for the maintenance of mitochondrial function and metabolic homeostasis in females. Science Translational Medicine 8(334):334ra54.
[41] Yan, H., Yang, W., Zhou, F., Li, X., Pan, Q., Shen, Z., et al., 2019. Estrogen improves insulin sensitivity and suppresses gluconeogenesis via the transcription factor Foxo1. Diabetes 68(2):291–304.
[42] Schuur, E.R., Loktev, A.V., Sharma, M., Sun, Z., Roth, R.A., Weigel, R.J., 2001. Ligand-dependent interaction of estrogen receptor-alpha with members of the forkhead transcription factor family. Journal of Biological Chemistry 276(36):33554–33560.
[43] Kawakami, M., Yokota-Nakagi, N., Uji, M., Yoshida, K.I., Tazumi, S., Takamata, A., et al., 2018. Estrogen replacement enhances insulin-induced AS160 activation and improves insulin sensitivity in ovariectomized rats.

American Journal of Physiology. Endocrinology and Metabolism 315(6): E1296–E1304.

[44] Church, T.S., Blair, S.N., Cocreham, S., Johannsen, N., Johnson, W., Kramer, K., et al., 2010. Effects of aerobic and resistance training on hemoglobin A1c levels in patients with type 2 diabetes: a randomized controlled trial. Journal of the American Medical Association 304(20):2253–2262.

[45] Sigal, R.J., Kenny, G.P., Boule, N.G., Wells, G.A., Prud'homme, D., Fortier, M., et al., 2007. Effects of aerobic training, resistance training, or both on glycemic control in type 2 diabetes: a randomized trial. Annals of Internal Medicine 147(6):357–369.

[46] Lai, K.M., Gonzalez, M., Poueymirou, W.T., Kline, W.O., Na, E., Zlotchenko, E., et al., 2004. Conditional activation of akt in adult skeletal muscle induces rapid hypertrophy. Molecular and Cellular Biology 24(21):9295–9304.

[47] Guo, T., Jou, W., Chanturiya, T., Portas, J., Gavrilova, O., McPherron, A.C., 2009. Myostatin inhibition in muscle, but not adipose tissue, decreases fat mass and improves insulin sensitivity. PLoS One 4(3):e4937.

[48] Yadav, H., Devalaraja, S., Chung, S.T., Rane, S.G., 2017. TGF-beta1/Smad3 pathway targets PP2A-AMPK-FoxO1 signaling to regulate hepatic gluconeogenesis. Journal of Biological Chemistry 292(8):3420–3432.

[49] Bollinger, L.M., Witczak, C.A., Houmard, J.A., Brault, J.J., 2014. SMAD3 augments FoxO3-induced MuRF-1 promoter activity in a DNA-binding-dependent manner. American Journal of Physiology - Cell Physiology 307(3):C278–C287.

[50] Amirouche, A., Durieux, A.C., Banzet, S., Koulmann, N., Bonnefoy, R., Mouret, C., et al., 2009. Down-regulation of Akt/mammalian target of rapamycin signaling pathway in response to myostatin overexpression in skeletal muscle. Endocrinology 150(1):286–294.

[51] Ussar, S., Fujisaka, S., Kahn, C.R., 2016. Interactions between host genetics and gut microbiome in diabetes and metabolic syndrome. Molecular Metabolism 5(9):795–803.

